UCID-20164

Seismic Fragility of Reinforced Concrete Structures and Components for Application to Nuclear Facilities

Peter Gergely
Hollister Hall
Ithaca, New York

September 1984

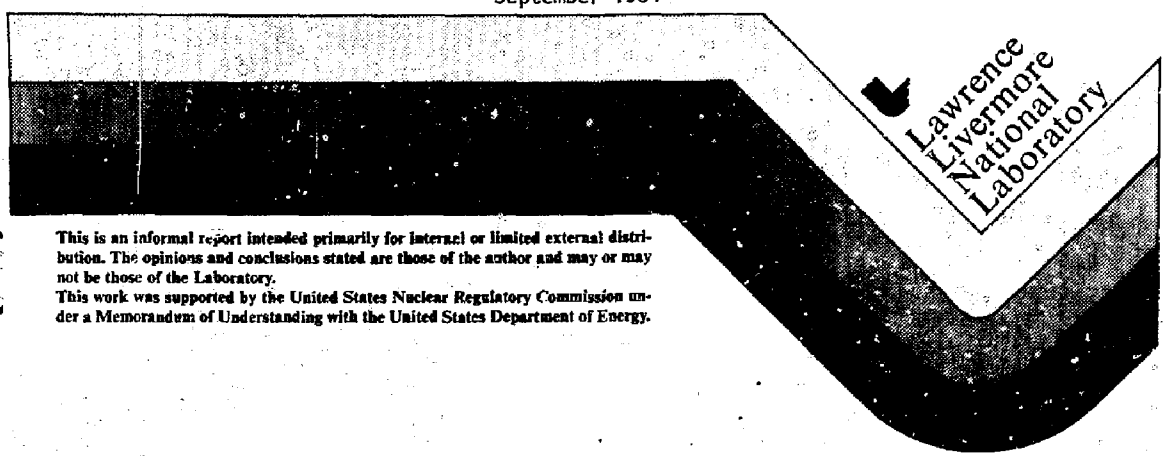

This work was supported by the United States Nuclear Regulatory Commission under a Memorandum of Understanding with the United States Department of Energy.

UCID--20164

DE84 017206

ABSTRACT

The failure and fragility analyses of reinforced concrete structures and elements in nuclear reactor facilities within the Seismic Safety Margins Research Program (SSMRP) at the Lawrence Livermore National Laboratory are evaluated. Uncertainties in material modeling, behavior of low shear walls, and seismic risk assessment for nonlinear response receive special attention. Problems with ductility-based spectral deamplification and prediction of the stiffness of reinforced concrete walls at low stress levels are examined. It is recommended to use relatively low damping values in connection with ductility-based response reductions. The study of static nonlinear force-deflection curves is advocated for better nonlinear dynamic response predictions. Several details of the seismic risk analysis of the Zion plant are also evaluated.

TABLE OF CONTENTS

LIST OF TABLES

LIST OF FIGURES

1 INTRODUCTION

Part of the Seismic Safety Margins Research Program (SSMRP) at the Lawrence Livermore National Laboratory has involved the determination of cumulative distribution functions of the probability of failure of critical elements or systems as a function of load levels. The primary purpose of this report is to evaluate the failure analysis used for reinforced concrete structures or elements. Most critical structural elements associated with potential undesirable accident consequences in nuclear reactor facilities are made of reinforced concrete.

The SSMRP encompasses a wide range of tasks, including detailed investigations of the earthquake hazard, soil-structure interaction, potential accident sequences, failure modes, dynamic analysis procedures, and failure probabilities. As described in Chapter 2, the key feature of the SSMRP is that uncertainties can be identified and their effects on the risk can be explicitly evaluated. Clearly, the knowledge of the levels of the various uncertainties is invaluable not only in the assessment of overall safety but also in pinpointing structural elements to be strengthened or modified.

For details of the risk analysis, this report relies almost exclusively on reports issued within the SSMRP (Ref. 1), especially on information contained in Ref. 2 which addresses the structural fragility investigation of the Zion Nuclear Power Plant. The behavior of only those reinforced concrete elements are studied here that were identified in the reports as being critical. It was obviously impossible within this limited effort to trace all conceivable failure sequences and check all steps of the SSMRP leading to the fragility analysis.

The expression "limit states" is used to denote any stage of behavior at which undesirable response occurs. Typical limit states are: cracking, yielding, drift, rupture, acceleration, crushing, and buckling. Any of these may control the design or the safety risk of a structure. In design one strives to avoid or delay undesirable limit states or those that are difficult

to predict but in risk assessment of an existing structure all limit states need to be considered without a chance to affect their relative levels.

Seismic design/analysis involves five major steps (Ref. 3): (a) identification of input, (b) idealization of the structure-soil system, (c) dynamic analysis, (d) interpretation of the results, and (e) establishment of safety factors or margins. Although the amounts of work required in these steps are different, each is important and difficult. For the purposes of this report, it is convenient to separate analysis from other tasks. Analysis dominates (c) but is also important in (a), (b) (soil-structure interaction), and (e) (fragility analysis in the present case).

Although dynamic analysis is very important and can demand huge amounts of time and effort, the other main elements of the design/analysis process that rely directly on material behavior, are also crucial. The principal feature of the SSMRP fragility analysis is that it provides better insight and the various steps are put in better perspective.

This report focuses on material behavior; on capacity, rather than on demand. Knowledge of the characteristics of various types of structural elements is required in steps (b) idealization and (d) interpretation of results. It is necessary to establish, explicitly or implicitly, the nonlinear characteristics of the structure on one hand and to judge the significance of the time-history of response on the other hand. Faced with the fact that the cyclic nonlinear benavior of reinforced concrete is highly complex and not fully understood, it is essential to rely on the judgement of experts who have developed years of first-hand laboratory experience in testing a variety of concrete structures. There are no shortcuts in this respect.

It is clear that material behavior, especially idealization of nonlinear behavior, cannot be divorced from analysis. Therefore, other aspects of the SSMRP are also discussed briefly in Chapter 2, and alternative approaches are mentioned in Chapter 4.

The main problem in earthquake resistant design and in analysis is how to account for nonlinear behavior that is inevitable during a major earthquake. Nonlinear dynamic analysis is resorted to only in very special cases, and it is often hampered with greater uncertainties than alternative approximate methods of including nonlinear effects. The approach used in SSMRP is discussed in Chapter 2, and several other methods are mentioned in Chapter 4 that might complement the current SSMRP analysis. A definite conclusion on which method is preferable is yet impossible, especially in the case of analysis rather than design.

Energy absorption greatly affects response but its primary forms, namely damping and hysteresis, are both functions of load level, cracking, and the load transfer mechanism. Moreover, viscous damping and ductility-based response reduction are interrelated in tests of reinforced concrete. These important questions are explored in Chapter 2.

The critical concrete components in the Zion Plant seismic risk analysis are the shear wall between the auxiliary and turbine buildings, and the roof of the crib house. Since shear walls are important in most nuclear plants, special emphasis is placed on shear wall capacity and behavior in this report. The specific design in the Zion plant and the fragility analysis within the SSMRP are examined in Chapter 3. Moreover, the more general question of shear wall behavior, aside from the particulars of the Zion Plant, are discussed. Validation is based on the state of the art, first-hand experience, and direct input from noted scholars in the US, Japan, and New Zealand.

A conscious effort is maintained in this report to offer new data or ideas for the improvement of fragility analysis. Unfortunately, there are several instances where one can only state or prove that current assumptions or values are questionable, but more accurate information must await further research.

The basic dilemma is that most information in earthquake engineering is on the design side, that is, how to proportion a safe structure. The answers need to be on the safe side and the main questions are only the difficulty of construction and the cost. On the other hand, the evaluation (analysis) of

existing facilities is much more difficult and has received some attention only lately. If the evaluation is concerned not only with the safety of the facility but, more importantly, with the safety margins and fragilities, the task becomes much more complex. Not only a lower bound of the test data is desired but also a best estimate as well as, in this case, the statistical variations.

In summary, this report examines and evaluates the following aspects of the SSMRP: the nonlinear idealization and behavior of low shear walls; the interaction of viscous damping and ductility-based reduced spectra; energy absorption and deterioration levels; the failure mode of the main wall in the Zion Plant; the analysis of pierced roofs; and a brief summary of methods of accounting for nonlinear behavior.

Acknowledgements

Many individuals were consulted during this study to discuss ideas, specific questions, or collect test data. This report has benefited greatly from this valuable input but only the author is responsible for its contents, especially for claims and conclusions. He is grateful to the following colleagues for stimulating discussions or communications by mail: A. Aktan, H. Aoyama, A. Banerjee, V. V. Bertero, B. Bresler, W. G. Corley, S. A. Freeman, J J. Johnson, J. G. MacGregor, S. Mahin, I. Martin, J. Moehle, P. Mueller, R. G. Oesterle, S. Otani, T. Paulay, M. Saiidi, M. A. Sozen, and D. A. Wesley. The nonlinear finite element analysis of the wall with studs was performed by W. Gerstle.

2 CURRENT METHOD OF FRAGILITY ANALYSIS

2.1 Introduction

The SSMRP analysis method comprises several major steps as summarized in the next section. Those that are dependent on material properties are examined in detail in this chapter, with emphasis on reinforced concrete. The discussion covers the method in general, whereas Chapter 3 is limited to an exploration of its application to the Zion plant.

The direct consideration and assessment of uncertainties in failure prediction are the principal objectives of SSMRP. Additional uncertainties in material modeling not yet included are presented in Section 2.5 based on recent test results.

The consideration of material aspects cannot be entirely divorced from the associated aspects of analysis methods. Therefore, this chapter includes comments on the prediction of response in SSMRP. In particular, the dilemma of linear versus nonlinear analysis is an ever present question facing engineers and is at the heart of the difficulties in SSMRP. Therefore, in Section 2.4 special attention is paid to the use of ductility factors and damping in the analysis.

2.2 Key Features of the SSMRP

The SSMRP is an ambitious program for the analysis of the uncertainties in the prediction of the risk of accidents caused by earthquakes. It has many facets, including the analysis of seismic risk at the site, identification of numerous accident sequences, determination of failure modes of a wide variety of components, response prediction, construction of fragility curves, and computation of accident sequence probabilities (Ref. 4). Some of these steps, particularly the soil-structure interaction, have entailed extensive reviews and significant advancements of the state of the art.

It is obvious that the SSMRP encompasses a wide variety of exceptionally complex tasks. An enormous amount of computations was necessary to evaluate the effects of numerous variables and their variations. The value of the program lies not only in the prediction of the uncertainties, which is in itself an important design tool, but also in revealing inadequacies in knowledge and systems.

Material (structural) properties are reflected in the idealization of the structure (stiffness, mass, damping) and in the analysis of failure (fragility) of elements. Both aspects are discussed in this chapter. A fragility curve represents the cumulative distribution function of the probability of failure for a given value of load (input).

A typical fragility curve is shown in Figure 2-1. The horizontal axis reflects the level of loading, usually represented by acceleration. There are two ways of specifying the load: it may be the free-field ground acceleration, or a response acceleration at a specified point in the structure. In the former case the curve is more directly usable but the entire response calculation (including soil-structure interaction) is coupled to the fragility curve. Also, the well-known problem of what ground motion parameters to use is present.

In the second approach the horizontal scale is a measure of the local response. The partial separation of the two main steps of the risk analysis is convenient and reduces the amount of computations. However, complete uncoupling is impossible because the internal forces, stresses, and strains in the element in question do depend on the response of the entire structure. In particular, the local response is strongly affected by damping and nonlinear behavior of the entire structure. Modal superposition at the structure level and the local response reduction are not really independent.

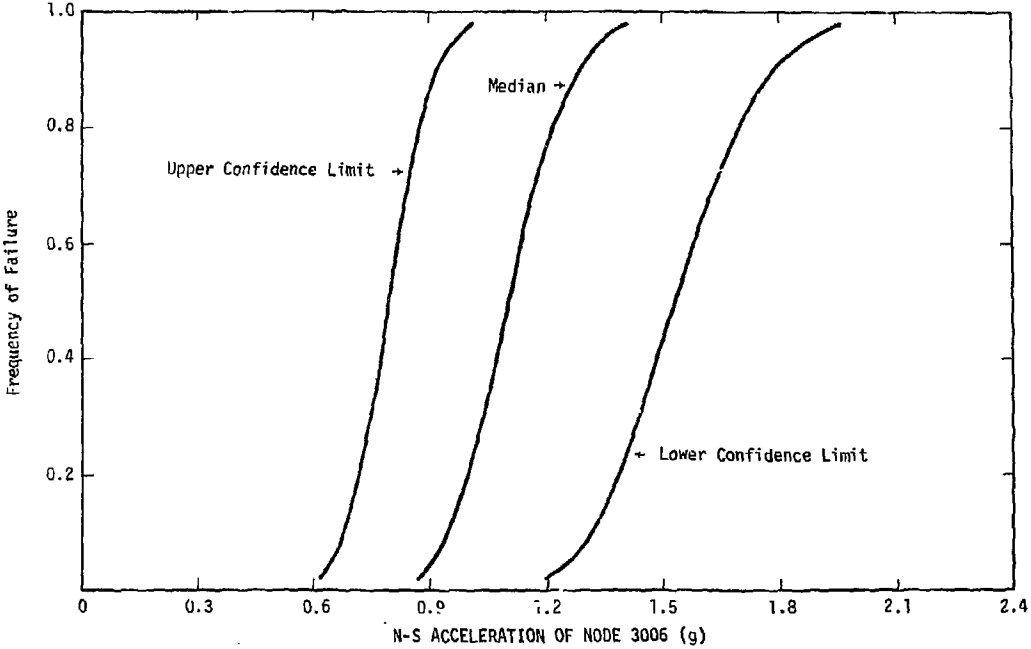

Fig. 2-1 Typical Fragility Curves

In the SSMRP local response parameters are used. The corresponding stresses in the critical element are calculated for a selected subset of the ground motions. This is a simplification that is justifiable, particularly if the response of the structure and the element remain linear.

Most fragility curves for local response are rather steep. This means that a small change in the input (local response) results in a large change in the probability of failure. This would be typical in very simple chain-type structures for which there are few uncertainties. For structures with complex geometries and combinations of materials, the fragility curves are expected to be flatter. In fact, one may state that, in general, the flatter the curve, the better is the design. This question is explored further in the next section.

The tail ends of the fragility curves also provoke questions. What is the importance of a very low probability of failure at very low input levels? What is the significance of high probability of failure at very high input levels? Clearly, such high accelerations may not be transmitted through the soil but large amplifications in the structure are possible. A cutoff of at least the upper tail may be advisable.

2.3 Limitations of Risk Analysis

The detailed probabilistic analysis of seismic risk is a monumental and important task. There are several complex questions involving seismic input, soil-structure interaction, idealization, systems analysis of accident causes and sequences, assessment of failure modes, nonlinear effects, overall and local behavior, just to mention the most obvious ones. It is not surprising, therefore, that a number of assumptions had to be made; most of these have been recognized and acknowledged (Refs. 1 and 2).

It should be pointed out that even if an assumption seriously affects the shape and values of the final fragility curve or risk assessment, the analysis may still yield important qualitative and quantitative information on the

uncertainties and effects of parameters. This section is devoted to a review of some of the assumptions related to nonlinear behavior and idealization.

Before discussing the main hurdle, nonlinear response analysis, a few comments are in order regarding even the linear idealization of fixed-base uncracked reinforced concrete structures. Unless many finite elements are used to model walls and floors, shear lag can distort simple analyses of low walls. For example, the flexural stresses in a low box are far from being linear (Fig. 2-2). Similarly, the shear stiffness of the shear walls is significantly affected by the proportions. This factor is important in structures common in nuclear facilities; the deviation from the prediction by simple bending theory can be over 100%. Other uncertainties in idealization are mentioned in Section 2.5.

The second observation regarding linear idealization concerns the inclusion of nonstructural filler walls. It is customary to exclude these walls from stiffness calculations although their masses are considered. It has been found that even unreinforced masonry walls can add significant stiffness (of the order of 50%); in particular they can affect the torsional stiffness, depending on their locations. It is often argued that their omission is on the safe side because increased stiffness would mean lower forces in very stiff structures which are on the low-period side of response spectra. That point is valid if one simply wants to be on the safe side. But a probabilistic risk assessment tries to predict the mean value of response and the error of 20% to 30% in the natural periods (probably more in higher modes) may significantly influence the analysis. The early failure of these walls may reduce this error but possible extant torsional vibrations and perhaps the transfer of kinetic energy could aggravate the response. Of course, the failure of nonstructural block walls may in itself be a limit state if critical equipment can be made inoperative.

It is essential to view response at several levels, including the most important one at collapse. Nonlinear effects become influential at rather low levels. Some of the manifestations of nonlinearity in buildings are: reduced

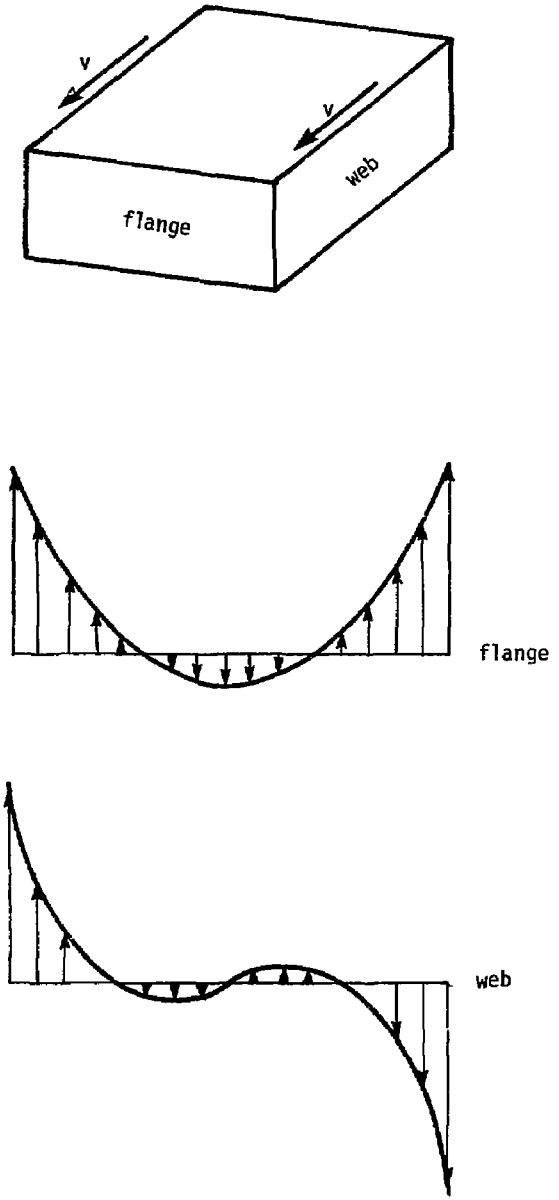

Fig. 2-2 Laterally Loaded Box Structure and Vertical Stresses

stiffness, increased damping and hysteretic energy absorption, load redistribution, and geometric (e.g. p-delta) effects.

The consideration of nonlinearity is, without any doubt, the most difficult question in SSMRP and in earthquake engineering in general. Experts agree that none of the approaches is entirely satisfactory and that they are more suitable for design than for analysis. At the same time it is obvious that nonlinear effects must be accounted for, explicitly or implicitly, in rational design/analysis for severe earthquakes; some approaches are summarized in Chapter 4.

Linear time-history analysis is used in the SSMRP, and the results are scaled down as in ductility-based reduction of response spectra. Obviously, the large number of input motions (180), the even larger number of accident sequences, and the complexity of the structure prohibit direct nonlinear analysis to evaluate all combinations. In fact, that approach is not more reliable (see Chapter 4). It is not the purpose of this discussion to propose another method of analysis but to point out the difficulties and uncertainties based on recent views and opinions. This will lead to future improvements, some of which are presented in Chapters 4 and 5.

The key to the survival of structures subjected to extreme loads is force redistribution. The collapse load is much higher than the load causing local distress in most structures. A good design and even more so a rational analysis, must account for this excess capacity. A thorough limit (collapse) analysis would be too complex in most cases (see Chapter 4) but an assessment of the behavior beyond the first distress (limit state) is important. This could be done for static loading.

Normally structures with a weak link should not be built. The loss of capacity of one element should not lead to collapse. To investigate this possibility, it is advisable to calculate the second line of defense. This can be done without a full limit analysis (Chapter 4).

There might be exceptions in nuclear power plants where loss of a critical element is fully equivalent to total failure. In that case the system is chain-type, and failure is brittle. For example, the relative displacement between the containment shell and auxiliary building may be excessive and constitute a failure limit state even for linear behavior of structures. These types of system failures are exceptions to the rule; if structural distress is involved, the second line of defense should always be investigated. In the probabilistic sense the second line may sometimes be the more critical and controlling limit state. Ignoring the response subsequent to the predicted failure of the weakest link is contrary to good, modern structural engineering.

The difficulties with the weakest-link approach are acknowledged in Ref. 2: "Some potential modes of seismic failure involve only a localized failure of the structure while others include the entire building. Based on the elastic load distributions used, less confidence exists for capacities of modes of failure which involve sequential failure of a structure."

Another difficulty with using linear analysis to predict nonlinear behavior is that different types of ground motions may be critical for nonlinear systems. Several studies have recently shown that long acceleration pulses in the ground motion can be very important for certain nonlinear systems but not for linear structures (Ref. 5). Such pulses often occur in near-field motions and are especially significant for low-period systems for which the pulse duration may be greater than the period. Conversely, the amplitude of the acceleration spikes, not necessarily the peak ground acceleration, are significant for linear systems but not for inelastic structures. The duration of the ground motion also affects mainly nonlinear systems.

Maximum inelastic response depends primarily on the largest velocity increment and the duration of the ground motion. The variation in response is large even for similar spectra. Therefore, the prediction of nonlinear response based on modified elastic spectra is a poor approximation, especially in the acceleration range of the spectrum into which nuclear structures belong (Ref. 15).

It is yet impossible to specify the critical characteristics of ground motions for various types of structures but it seems that currently used artificial ground motions are not appropriate for nonlinear analysis. Also, scaling of ground motions does not reflect the different properties of ground motions at various intensities. The linear analysis in the SSMRP avoids these problems.

Some light has recently been shed on the role of acceleration pulses (Ref. 6). If the system contains an element or subsystem (such as a story) with elasto-plastic resistance, the acceleration pulse (jump in velocity) causes a large permanent displacement even for relatively low acceleration amplitudes. However, if the resistance always has positive nonzero stiffness (strain hardening), it is usually able to bring the system back and avoid large excursions. Nonlinear time-history analyses can reveal these differences which are particularly significant for high-frequency structures.

Damage and failure often are functions of the number of inelastic cycles which is greater for an El Centro type of long input. The energy input is much greater for the pulse-like Parkfield input, but the number of inelastic excursions is much smaller. The maximum ground acceleration is less important for the latter type of earthquakes (Refs. 7 and 10).

As mentioned previously, the local response (horizontal axis) of the fragility curves is not directly tied to ground motion in the SSMRP but the stresses in the critical elements are. Therefore, the question arises whether a linear time-history analysis can properly predict the force distribution and the failure of the element and the associated local response levels. The analysis must account for the frequency characteristics and amplifications of the nonlinear response.

It must be recognized and acknowledged that a thorough risk analysis of a nuclear facility is too complex to be carried through at present. The systems aspects involve manifold interactions of structural, mechanical, electrical, and chemical-physical elements. It is likely that human errors at their interfaces pose a greater risk than the failure of any subsystems due to specific causes.

2.4 Ductility and Damping

It is well known that both viscous damping and hysteretic energy absorption (ductility) can reduce the response significantly; therefore, both factors must be selected with great care. Unfortunately, the estimation of these factors is difficult, especially in cases where both are significant, and thorough studies of this problem have been conducted only very recently.

The effects of damping and ductility depend, among other factors, on the characteristics of the input and on the frequency of the system. For example, damping absorbs more energy than hysteresis for the El Centro earthquake, whereas the opposite is true for the Parkfield input (Ref. 7). The significant difference is the duration of the motion, a factor that is normally not accounted for in analysis. The number of inelastic excursions affects the response which depends not only on the duration but also on the properties of the system. Most of these effects are revealed only in nonlinear time-history analyses and not in linear or spectral analyses.

The construction and use of inelastic spectra received lots of attention during the past couple of years. These spectra are certainly useful in preliminary design but many unanswered questions must be resolved before it becomes a sufficiently reliable analysis tool (Refs. 5, 8, 10, 11, 15). Some of these uncertainties are discussed in the following paragraphs.

The main shortcoming of ductility-based spectra is that they do not sufficiently account for such time-dependent effects as deterioration, cumulative damage, duration of input, and the number and size of acceleration pulses. Since they are averages, ground motions with special characteristics are not reflected. It may be possible to generate such spectra for particular sites using accelograms with appropriate properties. Artificial motions do not, in general, possess these special features (for example, the large acceleration pulses often found in near-fault accelograms). It remains a question whether these factors can be reflected in linear analyses.

The most convenient approach is to construct the inelastic spectra from an elastic spectrum (Ref. 9). The amount of deamplification is different in the various frequency regions of the spectrum. It has been pointed out by several investigators that it is unduly conservative, in nearly all cases, to tie the spectrum to the peak ground acceleration. However, the various definitions of effective maximum ground acceleration differ considerably (for example, Refs. 7, 8, 10, 11, and 15). These differences affect the uncertainty analysis.

Some of the initial frequencies of the main structures in a power plant are in the transition range, 8 to 33 cps, of the Newmark spectrum. It is felt by some that the proposed straight transition between the constant acceleration region (above 33 cps) and the velocity region (below 8 cps) is not as reliable as the deamplification in other regions. This uncertainty should be examined.

The effect of damping on the inelastic spectra has recently been revised (Ref. 9), and the new values were used in the SSMRP analyses. However, for near-fault ground motions with large acceleration pulses damping has a different influence than for the previously used motions (Ref. 5). Thus, the construction of inelastic spectra and the reduction of stresses need to be modified for near-fault sites.

The error involved in the use of inelastic spectra in modal analysis is not known. Fortunately, the natural frequencies of the structures of interest in nuclear facilities generally fall in the acceleration region and higher modes are often not too important. Soil-structure interaction can lower the frequencies but not below the transition point at 2.5 cps. Therefore, the error is probably not great, but this problem needs further study. Higher modes are especially important if torsion is present. The question persists, nevertheless, whether it is proper to use the original frequencies with an inelastic spectrum, as it is currently done. The effective period shifts during inelastic response and the amount of shift may be an important variable, especially for stiff structures; this question has not been addressed.

In fact, it appears that the use of inelastic spectra is equivalent to and may be replaced by the elastic spectrum together with a period shift and increased damping to account for inelastic effects. Such an approach is attractive, at least for uniform structures, as it is explained further in Chapter 4.

This discussion focuses on material behavior and its effect on ductility-based analysis. The main questions are: the shape of the hysteresis curve, the value of ductility factor for the critical element(s), and the value of the average ductility factor for the structure.

The deamplification (reduction) due to inelasticity is not strongly affected by the type of hysteresis: elastoplastic, bilinear, or simple degrading (Refs. 9, 11). Since the spectrum reduction is a function of the hysteretic energy absorption, the change of the area under the hysteresis loops is of direct concern. The ductility (maximum inelastic excursion) may be equal for two systems, but the hysteretic energy absorption could differ considerably. Therefore, the reduction rules are not expected to be reliable for systems with small or varying hysteresis areas.

A hysteresis curve with a small area is shown in Fig. 2-3a. This shape (called pinched curve) is typical for systems with slip, sliding shear, or bond-slip. An indication of the amount of energy absorption is the value of equivalent viscous damping, which is of the order of 10 to 13% for stable elasto-plastic systems. For the shapes shown in Fig. 2-3a the equivalent damping is about 3.5% for a ductility in the range of 4 to 8 (Ref. 12). Tests on shear walls have shown that the equivalent damping may reduce to about 3% (Fig. 2-3b) after a few cycles (Ref. 13). Such reductions in energy absorption are not uncommon in reinforced concrete and were not included in the Newmark study.

A ductility factor of 4 was used for the shear walls in the SSMRP. This value is acceptable for typical tests in which flexure dominated the behavior and a reasonable gravity load was present. A smaller value is recommended for

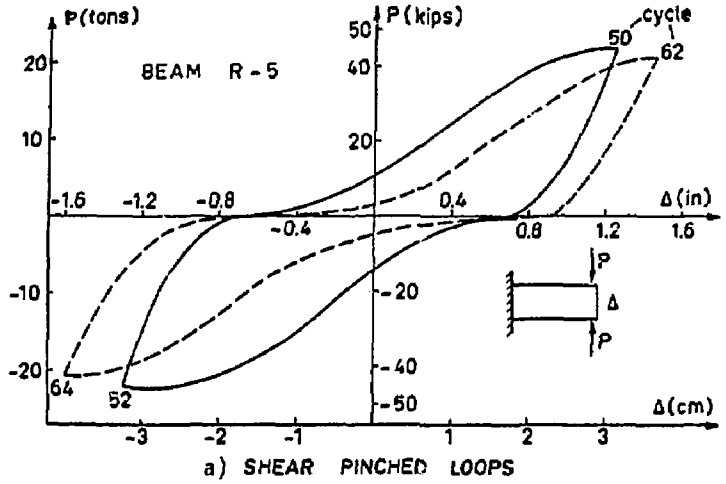

a) SHEAR PINCHED LOOPS

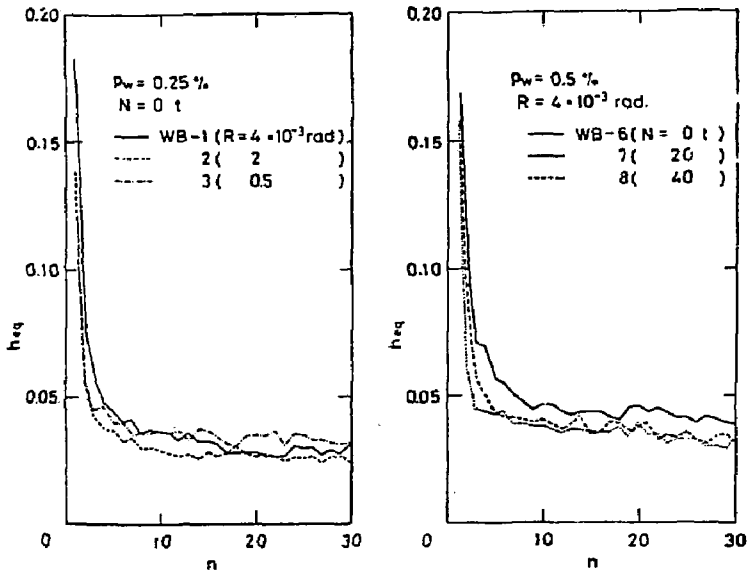

b) EQUIVALENT VISCOUS DAMPING

Fig. 2-3 Shear-Pinched Hysteresis and Equivalent Viscous Damping

low walls with a relatively small vertical load resulting in pinched loops; a ductility factor of 2 is reasonable. Well-confined concrete or steel columns reduce the ductility as they may facilitate the creation of a stiff truss mechanism. In this case the reduced ductility factor is not a measure of the maximum displacement, which can be large when slip is present, but of the diminished hysteresis area. Also, the coefficient of variation of 0.18 based only on the PCA tests and adopted in Ref. 2 is low for use in the general case. Another fact to be considered is the larger number of inelastic cycles (8 to 10, at least) of stiff structures in a major earthquake in comparison with about 4 to 6 cycles normally taken for more typical structures; these differences are important in adopting test results.

Even if one can estimate the ductility for the critical weakest element or subsystem, it is much more difficult to estimate the system ductility. As it is acknowledged in the SSMRP (Ref. 2): "The assumption made in this investigation is that the average or system ductility expected will be close to the story ductility ratio for well-designed structures. For buildings with large localized ductilities, however, this assumption can be nonconservative." But the same problem holds even within a story if several dissimilar elements share in carrying the load; a static nonlinear analysis would greatly aid in estimating the system ductility.

In fact, in the auxiliary-turbine building complex the story between elevations 592 and 617 ft yields first and much more than the other stories for several inputs scaled to ductility levels of 1, 2, 3, and 4 (Ref. 72). For such a nonuniform resistance the ductility-based spectrum prediction using the maximum story ductility was found to overestimate significantly the reduction in acceleration response. Several schemes have been proposed to take into account local nonlinearities in modal analysis (for example in Ref. 73) but their validity for a wide variety of situations needs further studies.

In Ref. 2 the wall ductility of 4 was reduced to a system ductility of 2 (page 3-12) with a COV = 0.18. However, in Appendix A the respective values are 2 and 1.2 (with a logarithmic standard deviation of 0.03) for the

east-west diesel generator building shear wall. Although the effect of a change in the value of ductility factor is smaller in the transition region than in the velocity region of the spectrum, the differences are appreciable and the uncertainty is large. Again, a nonlinear analysis (static or dynamic) would allow a better estimate of the system ductility because it would reveal the degree of inelasticity in various segments of the structure.

The ductility factor is inversely proportional to the yield deformation. Therefore, errors in the estimation of the elastic limit directly affect the value of ductility factor. It is usually difficult to define the beginnings of significant inelastic action; this is an appreciable source of uncertainty, especially for complex and stiff systems.

The local response (horizontal scale) of the fragility curves, as in Fig. 1, was derived from a set of elastic time-history analyses. Nonlinear behavior (ductility) was not accounted for at this stage of the calculations, and only the final element stresses were reduced for the fragility analysis. The effect of this approach on the fragility curves depends on the sensitivity of the element response (such as the shear wall stresses) on nonlinear system properties. This method is much simpler and is probably adequate; again a nonlinear analysis would be required to ascertain the dependence of element (wall) stresses and local response acceleration on system nonlinearities.

The input motions in the SSMRP were grouped into 6 levels (intervals) of acceleration. Although the fragility curves would probably not be affected much in the method adopted, both the ductility and the damping values should have been different for the different levels of input. This could be done without much additional effort.

The selected damping ratio of 10% is the highest value recommended by Newmark for reinforced concrete at or near yield levels. Test results at low free-vibration amplitudes have indicated much lower values even after prior damage. Free-vibration tests of nine walls (Ref. 14) produced the following damping percentages:

before cycling: 2, 2.2, 3.6, 3.4, 2.7, 5.5, 2.8, 2.9, 3.5.

after few cycles below yield: 9.8, 8.5, 10, 6.7, 9.6, 6.8, 9.4, 4.8.

after few cycles above yield: 9.1, 14.5, 8.5, 12.5, 11.

The averages are 3.2, 8.2 and 11.1%, and the COV's are 0.30, 0.22, and 0.20 for the three load levels.

Other tests of lightly cracked structures, including full-scale buildings, resulted in about 1.5 to 2% damping. Clean structures (without walls) exhibit relatively low free-vibration damping of only 5% even after extensive damage. Values quoted in Ref. 9 are: 1.2% low level, 5.7% (COV = 0.50) high level, from one source and 4.3% (COV = 0.76) low level, 6.6% (COV = 0.64) high level from another source. These are rather low values and the coefficients of variation are large.

There are several test results on reinforced concrete structures without nonstructural elements that confirm the above lower damping values. In recent tests at the University of California at Berkeley of a seven-story model the following values were measured: virgin model 1.4%, at cracking 3.7%, and after extensive yielding 6.9%. The maximum damping obtained after a large sliding-shear mechanism developed at the base of the wall was about 8%. Actually the level of damping would reduce if large forces open the crack and reduce the friction. Although these higher values were measured in low-level free vibration tests, some hysteresis was present, and therefore the high values should not be used in a ductility-based analysis.

A series of low and high-level forced vibration tests were performed on an 11-story reinforced concrete building with block walls in St. Louis (Ref. 28). Small-amplitude tests of several translational and torsional modes (15 measurements) gave an average of 1.6% damping with COV = 0.41. For a series of 16 loadings at large force levels producing some damage (crushing, spalling) the corresponding numbers were 3.9% and 0.40; if only the 8 tests

after damage are included, the values become 5.1% and 0.28. After the block and brick external walls were removed, 29 high-level tests resulted in 3.1% and COV = 0.28. All of these values are rather low and in reasonably good agreement with other measurements.

Acceleration measurements in numerous buildings during the San Fernando earthquake allowed the estimation of effective viscous damping. A plot of damping against the local ground motion represented by the zero-percent damping spectral velocity shows a reasonably linear relationship (Ref. 29). For reinforced concrete buildings the values range from about 1.5% at or below S_v = 10 in/sec up to about 12% at and above 45 in/sec. However, these measurements were probably influenced by soil-structure interaction.

Partial explanation for the differences between the Newmark (NRC) values and measurements is that Newmark's high damping values were based on judgment and were designed to account for hysteretic values in linear analysis. Therefore, the use of high damping together with nonlinear analysis or ductility-based response reduction amounts to duplication of hysteretic energy absorption. (In any case, even the equivalent damping values used to represent hysteretic behavior are of the order of only 6% to 12%). In all high-level tests of reinforced concrete which include hysteretic damping, the separation is impossible.

The level of damping to be used with nonlinear analysis has not been discussed much in the literature. It is clear, however, that damping should not include hysteretic effects. Ref. 9 states, "There is no evidence available indicating what degree of damping should be used when inelastic behavior is explicitly considered by means of a nonlinear resistance function. However, since in this case damping is meant to represent the energy dissipation associated with 'elastic' stages of response, it is reasonable to consider values corresponding to moderate stress levels, say about half the yield point."

Another point to be made in this respect is that in structures in which local nonlinearities develop, the damping would have to be averaged over the structure in some manner. Separation of hysteretic and damping energy absorptions avoids these difficulties with the selection of overall damping ratios. The hysteretic damping value may also depend on time because damage may not develop early in an earthquake.

Based on the above discussions, a mean value of damping of 4% is recommended with COV = 0.30. Fortunately, the effect of damping on the inelastic spectrum is not great in the acceleration region (above about 2 cps). The differences in deamplification for 5% and 10% damping are:

Damping | Ductility	2	4	6
5	0.560	0.386	0.317
10	0.606	0.426	0.354
ratio	1.08	1.10	1.12

Alternatively, using the values in Table 4.7 of Ref. 9, the increase in response due to using 5% rather than 10% damping is 2.28/1.78 = 1.28, with COV = 0.20. The differences are even less with significant soil-structure interaction.

Damping also affects modal combinations in response spectrum modal analysis; a recent study resulted in the combination rule shown in Fig. 2-4, which indicates three methods of superposition (Ref. 3). The derivation was for stationary Gaussian random inputs with a flat spectrum in a risk-consistent analysis. The superposition depends on the ratio of frequencies λ, the fraction of damping ξ, and the correlation coefficient of the modal coordinates

$$\rho = \frac{8\,\xi^2\lambda\,\sqrt{\lambda}}{4\xi^2\lambda\,(1+\lambda) + (1+\lambda)(1-\lambda)^2} \quad . \qquad (2\text{-}1a)$$

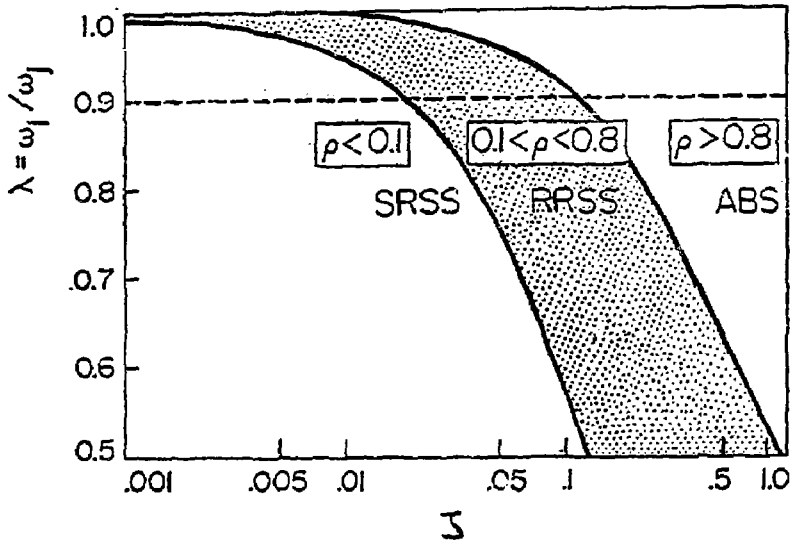

Fig. 2-4 Modal Superposition Rules with Consideration of Damping (Ref. 3)

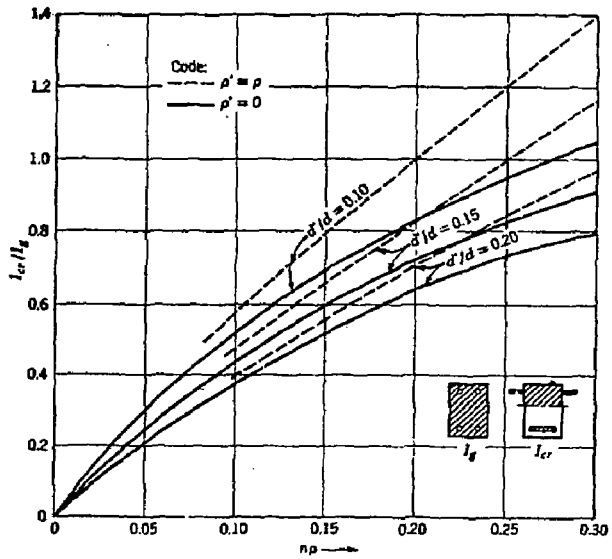

Fig. 2-5 Ratio of I_{cr}/I_g for Rectangular Sections Having d' = h-d

The proposed RRSS rule should be used in certain regions as indicated in the figure; then the superposed response value R_s for modes i and j is

$$R_s = \sqrt{R_i^2 + R_j^2 + 2\rho R_i R_j}. \qquad (2\text{-}1b)$$

Note that this rule is between the SRSS rule ($\rho = 0$) and the ABS rule ($\rho = 1$).

The effect of damping is revealed in the figure: the absolute superposition need not be used for little damping, and the SSRS method is unconservative for large damping even for widely separated frequencies. The method is sensitive in the $\lambda > 0.9$ range, and neither the ABS nor the SRSS method is accurate in the $0.1 < \rho < 0.8$ range.

Current approximate methods of combining responses for two independent orthogonal ground motions are generally conservative. It has been found, however, that inelastic response to multicomponent ground motions is worse than the combination rules derived for linear response. This problem has not been studied for complex systems with gradual loss of global stiffness.

2.5 Uncertainties in Material Properties

The effects of variations in the strength and stiffness of materials on seismic risk was considered in the SSMRP. The relevant properties of concrete and steel, and the errors in stiffness predictions are examined in this section.

There are several types of uncertainties affecting the effective concrete strength to be used in analysis (Ref. 16). The variation of cylinder strength depends on quality control and on the strength of concrete. A normal

distribution may be assumed with COV = 0.10 for concrete compressive strength above 4000 psi and better than average quality control.

The in-situ strength is less because of casting conditions, larger volume, water migration, and inferior curing. These factors were not considered in the risk analysis of the Zion plant. Based on core sample tests, the in-situ strength was found to be about 0.74 - 0.96 times the cylinder strength with an average of 0.87. For good curing a value of 0.90 may be used. However, the cores were typically taken from slabs which are easily vibrated and shallow. The covariance factor is about 0.20 (Ref. 71). A greater reduction is expected in deeper members congested with steel bars as in the containment wall; but no information exists on this.

The following formula has been suggested for in-situ concrete mean strength (Ref. 16):

$$f_{cs} = 0.675\, f_c' + 1100 < 1.15\, f_c', \qquad (2\text{-}2)$$

which gives f_{cs} = 5500 psi or 0.84 f_c' for the 6600 psi concrete in the Zion plant.

Aside from the moisture problem, volume also affects concrete strength because the probability of flaws increases with volume. As the volume grows to infinity, the mean strength approaches 0.58, but the COV diminishes. It was found (Ref. 16) that volume has a negligible effect on the minimum strength. A reduction would be appropriate for the heavy shear walls; the formula

$$f_{cv}' = f_c' \left[0.58 + 0.42 \left(\frac{64}{V} \right)^{1/3} \right] , \qquad (2\text{-}3)$$

where the volume V is in $in.^3$, gives about 0.60 for a portion of the wall. The variation is only

$$COV = \frac{0.147\ (64/V)^{1/3}}{0.60} = 0.0075$$

However, the reduced local compressive strength would not affect the strength of the entire reinforced wall; but such a reduction may be used in the strength formula (Section 2.6) which estimates the mean strength.

The effective compressive strength is also reduced by the existence of transverse tensile stresses and strains. For example, the diagonal crushing capacity is reduced significantly by the diagonal tension in a panel located in shear (Ref. 17). More is presented on this factor in Section 2.6.

The rate of loading influences the concrete strength; the increased stress is

$$f_{cr} = 0.89\ f_c'\ (1 + 0.08 \log r), \qquad (2\text{-}4)$$

where r is the loading rate in psi/sec. To get a rough idea of the increase, if a stress of 600 psi is reached in 0.10 sec during the earthquake-induced vibration of a stiff structure, r = 6000 psi/sec and $f_{cr} = 1.16\ f_c'$. The COV was found to be negligible.

The shear strength of concrete has been related to the tensile strength of concrete. Ref. 16 recommends the following expressions for the tensile strength.

$$\text{split cyclinder strength } f_t = 6.4\ \sqrt{f_c'} \qquad (2\text{-}5)$$

$$\text{modulus of rupture } f_t = 8.3\ \sqrt{f_c'} \qquad (2\text{-}6)$$

In the case of walls, the split cylinder strength is a better measure of the diagonal tension cracking strength. If the compressive strength is used in a formula to estimate the tensile strength (e.g. by the above formulas) and not by direct measurements, the COV's are 0.13 and 0.20. Otherwise the variations in direct measurement are 0.067 and 0.063.

The in-situ variability in tensile strength is to be estimated from the variation of f_c' in the above equations because direct test results are not extant. The effect of rate of loading is somewhat higher in tension than in compression; a factor of 1.20 is recommended.

Several new expressions have been proposed for the modulus of elasticity of concrete in compression. The well-known expression

$$E_c = 57{,}000 \sqrt{f_c'} \tag{2-7}$$

has been used in the SSMRP. The coefficient was recently modified to 60,400 in Ref. 16 to predict the initial tangent modulus with COV = 0.08. The equation

$$E_c = 40{,}000 \sqrt{f_c'} + 1(10)^6 \tag{2-8}$$

was recently recommended in an unpublished study for high-strength concrete. For a 6600 psi concrete the above three expressions give 4630, 4910 and 4250 ksi. The last is probably the best for f_c' greater than 6000 psi. However, the role of E is greatly reduced as a result of cracking as will be explained in the following.

The variation of steel strength is ordinarily more important than the variation of concrete strength because capacity is related mostly to steel strength. The variability of yield stress was evaluated in the SSMRP, but several observations are in order.

The yield strength of steel appears in capacity equations for flexure, shear and axial force. However, in most cases the capacity is appreciably greater if sufficient local ductility is present to strain the steel into the hardening region. This is likely at flexural hinges but not for shear failures. The strength of steel is normally taken about 1.3 times the yield strength.

The analysis in the SSMRP and in the reference used therein lump all bars No. 3 to No. 11 together. Yet smaller (No. 3-No. 5) bars have somewhat higher strengths than larger bars, and the difference would affect the analysis of structures dominated by walls which usually have small bars.

The tensile strength of steel bars embedded in concrete is higher than the coupon strength. The latter fails at the weakest spot anywhere within the test length. However, an embedded bar is highly stressed only at and near cracks and the probability of having the weak spots at cracks is less than one. Therefore, the statistical yield and tensile strengths of bars in concrete are greater than the coupon values. Tests to failure of reinforced concrete tension members would give the desired information but a limited search has not revealed any useful data.

One can estimate the effect of embedment on the probability of failure by calculating the total length of a bar that is highly stressed. The crack spacing at and above yield is about $2t_c$, where t_c is the cover measured to the center of bars. The highly stressed portion of the bar extends about two diameters on either side of the crack. Therefore, the fraction of failure prone length of the embedded bar is about

$$\frac{2d_b}{t_c}. \qquad (2\text{-}9)$$

In the remaining portion of the bar between cracks the stress can be assumed to decrease linearly to zero at the centerline. By assigning

probabilities of failure over segments of the bar between cracks, depending on the stress levels, a reduced overall probability of failure can be estimated.

The increase in yield strength for rapid loading is

$$3.2 + 1000\ r \qquad (2\text{-}10)$$

where r is the strain per second (Ref. 18), with a maximum of $r = 0.0016/sec$. For a wall structure the fundamental frequency is relatively high and results in a higher rate; therefore the limiting value gives an increase of 4.8 psi as opposed to a decrease claimed in Ref. 2.

It should be noted that the rate of loading on the strengths of concrete and steel is a major factor in small model testing because scaling laws require high frequency loading. The increase in material capacity must be considered in the evaluation of small model tests.

The most significant uncertainty in the response analysis of low shear-wall structures for a given input involves the estimation of the stiffness, especially at the relatively low stress levels expected in the heavy walls of the auxiliary and turbine buildings. Even for high-level loads, modal analysis using inelastic spectra is also based on the initial frequencies. Several sources of uncertainty are examined in the following.

One question is the effective width of floor slabs to be included with beams. Codes specify various widths depending on the dimensions (slab thickness, span and beam spacing) for monolithic concrete or composite steel/concrete construction. Recent finite-element analyses and evaluation of experiments have indicated that larger effective width can be used, as large as the distance between slab centerlines. The latter value is recommended, unless the span is short, until a detailed study is made. The moment of inertia and consequently the natural frequencies are strongly dependent on the effective width in frame structures but much less in wall structures.

The initial and low force-level stiffness of concrete structures are greatly affected by shrinkage and thermal cracking. A thorough study of published and unpublished data has revealed a wide variation in the reduction of stiffness, especially for wall structures. It seems that the two main factors that must be considered are: the size of the structure tested and the curing or handling conditions. The following is an attempt to summarize this effect.

Available test results can be grouped as follows:

1. Very small scale: 1/30, LANL
2. Small scale: 1/10, LANL, U of I
3. Medium scale: 1/5-1/2, UCB, PCA
4. Full scale: Japan, various structures in LA

Shrinkage strains are inversely proportional to the thickness of the element. Curing and handling are equally important and their effectiveness also depends on the thickness. For example, the time of removal of the forms is a main factor. The amount of restraint provided by the forms strongly affects shrinkage stresses and this depends on the shape of the section. For instance, the side forms on the web of an I Section restrain shrinking.

Delaying the removal of forms and extended moisture-curing can make a great difference in the final shrinkage strains. Thus the study of experimental data, as well as prediction of this factor, must consider the details of construction. Another complication is that shrinkage cracks can heal if ample moisture is continuously present for an extended period.

Shrinkage stresses develop only if a restraint is present. Aside from the form, the other source of restraint is the reinforcement. A variety of tests and calculations have shown that shrinkage effects increase with the reinforcement ratio. A thicker element (column) with less shrinkage can also provide the restraint necessary to induce stresses and cracking in walls.

As expected, the very small (1/30 scale) models showed the greatest differences between predicted and measured stiffnesses or frequencies. The ratios of measured to predicted stiffnesses ranged from 0.29 to 0.36 (Ref. 19); the frequency ratios are the square roots of these values. The reinforcement ratio was high (0.58%) which causes more shrinkage stresses. Shrinkage cracks were not visible in these tests but the small size of the models made it difficult to detect cracks; probably even with a magnifier. The box-shaped 1/30 scale tests had stiffness ratios of 0.24 and 0.18. An additional factor that might explain the low shear stiffness is the shear lag effect as described earlier in this chapter.

It is doubtful that microconcrete or another material for use in small models can be found that properly simulates not only the stress-strain characteristics of regular concrete but also the volume-change properties due to shrinkage and temperature. This deficiency seriously limits the usefulness of small models if stiffness, especially shear stiffness, at low stress levels is to be measured.

The stiffnesses of the 1/10 scale wall-frame tests at the University of Illinois were reasonably well predicted (within about 10%) using the cracked section properties. The ratio of cracked to gross flexural stiffnesses depends on the amount of steel (see Fig. 2-5 from Ref. 20) and is usually about 0.4 to 0.6. It also depends on the level of axial force. For relatively high vertical loads due to the added masses, the measured frequency was 86% of the predicted value using gross section properties; the range was 0.83 to 0.89 (stiffness ratios of 0.69 to 0.79).

In these tests, and in other tests where the measured to predicted ratio is relatively high, some low-level cycling reduced the ratio of frequencies to the 0.40-0.50 range. The change in frequency with seismic input is illustrated in Fig. 2-6 (Ref. 21). These tests and others reported in the following show that minor loading added to existing shrinkage stresses can produce appreciable cracking. The shear stresses at diagonal cracking in

small shear panels tested at the University of Toronto depended strongly on the age of concrete and therefore on the amount of shrinkage stresses; the range was 4 $\sqrt{f_c'}$ to 6 $\sqrt{f_c'}$ (Ref. 58).

Careful measurements on 1/3 scale frame-wall structures indicated a strong dependence of the stiffness reduction on the vertical load which may limit shrinkage cracks (Ref. 22). Measured shrinkage strains increased linearly to about $350(10)^{-6}$ in 80 days. For zero vertical stress the stiffness ratio was about 0.40 during initial loading and reduced further with some low-level cycling which induced some cracking, approaching the cracked stiffness (a ratio of about 0.35 to the gross section stiffness). The shear stiffness was also measured and gave ratios of about 0.7 initially but only 0.52 during the second low-level loading. After several cycles the ratio reduced to 0.10. These ratios were much higher (up to unity) as the vertical compression increased.

Vertical stresses caused by the weight of upper stories greatly increased the shear stiffness as cracks were closed or reduced. A moderate stress of about 200 psi increased the combined shear and flexural stiffness by 30%; this vertical stress was applied externally to simulate 11 stories above the bottom four stories modeled in the test. Even the ballast used for scaling purposes can make a difference. In the 1/5 scale model at Berkeley the stiffness increased by 40%.

If tension is present in a wall, for example due to pressure in a containment or a room of the auxiliary building, the shear stiffness is drastically reduced because cracks open. An effective shear modulus of as low as 0.06g was found experimentally (Ref 23). This is much less than the 0.5g that is often assumed.

Tests in Japan of box and cylinder structures with wall thicknesses of 3.10 and 3.93 inches also resulted in stiffness ratios of about 0.56 to 0.67 (Ref. 25). The differences were blamed on shrinkage microcracks and less than full effective width of flanges. A much closer agreement was possible when

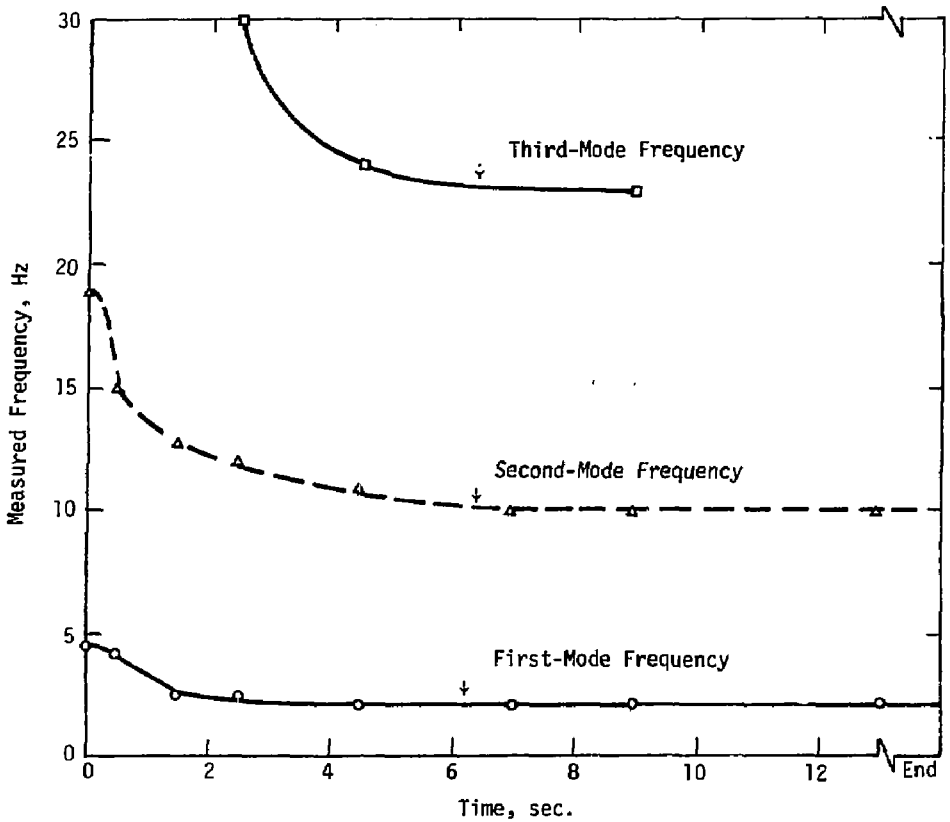

Fig. 2-6 Changes in Apparent Frequency During First Test Run (Test Structure M)

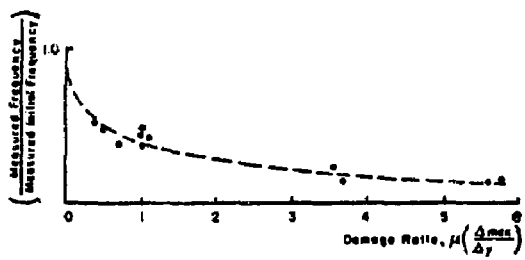

Fig. 2-7 Variation of Measured Fundamental Frequency with Damage Ratio

the tension concrete due to flexure was ignored in the flexural stiffness calculations. The measured stiffness was lower for specimens with higher steel percentages in which greater shrinkage stresses developed.

The eight isolated wall panel tests at PCA resulted in an average measured/calculated frequency ratio of 0.75 with COV = 0.066. Its square, the average stiffness ratio was 0.56 with COV = 0.126 (Ref. 14). These were 4-inch-thick walls, 15-feet high and very carefully cured. Also, the forms were left in place for longer than usual. An indication of the importance of forms in reducing shinkage is the fact that after only one side of the forms was removed, the wall began to curve noticeably due to unsymmetric shrinkage.

In a recent reevaluation of the PCA data the shear deformations and a more accurate calculation of the effective shear areas of flanged walls (which were as low as 0.52 times the full area) were considered (Ref. 25). With these improvements the average frequency ratio was 0.91 with COV = 0.071. These numbers include one test with more initial cracking due to shrinkage and handling for which the frequency ratio was considerably lower - 0.76. The stiffness ratios, calculated as the squares of the frequency ratios for all 8 tests give a mean value of 0.84 with COV = 0.133.

It is of interest to note that even modest loading, to less than half the yield level, reduced the frequency to about half the initial measured frequency (and therefore to about a quarter the stiffness ratio) as shown in Figure 2-7. A similar plot shows the increase of free-vibration damping from 2-4% to 7-12% as the damage ratio increases from zero to one. This study shows that if shear flexibility and effective shear areas are properly accounted for, a stiffness ratio of about 0.80-0.85 can be obtained for carefully cured specimens.

Stiffness ratios for full-size structures are not readily available, mainly because of the lack of predicted values. The full-scale tests in Japan as part of the U.S.-Japan cooperative program showed that the initial frequency reduced by 50% after "microtremors". Several ambient vibration measurements

on multistory concrete buildings indicated a reduction of frequency to almost 0.3 to 0.6 as a result of the San Fernando earthquake of 1971 which caused minor cracking in these structures. Other studies also showed that the period doubled after minor shaking; however, all of these were actual buildings with many nonstructural elements. Also, soil-structure interaction, especially rocking, can account for most of the reductions.

A comparison of the full-scale tests in Japan with the 1/5-scale test at Berkeley (Ref. 26) points out the difficulties with reduced-scale dynamic testing. Some of the problems found were: use of microconcrete with required stress-strain, tensile strength, and shrinkage properties; greater strain gradient in the model; larger loading rate; higher statistical steel strength in the model; and different bond characteristics. The stiffness deterioration was much quicker in the prototype. For the full-scale test frequency reductions were 22% after the 0.107 g Miyagi-Oki input and a total reduction of 63% after the subsequent Taft input at 0.327 g. The stiffness of the 1/5-scale model reduced 28% after the application of a 0.097 g level Miyagi-Oki shaking and a total reduction of 45% after additional input at 0.147 g and 0.247 g of the same motion.

The change in period after minor and significant earthquakes is depicted graphically in Fig. 2-8 for two seven-story reinforced concrete buildings located 13 and 23 miles from the epicenter (Ref. 27). The periods doubled as a result of the damaging motion. One must be careful in judging frequency reductions in actual buildings because soil compliance may be a major cause. Likewise, laboratory tests may also be affected by support flexibility. This factor was eliminated or accounted for in all or nearly all of the test results reported above.

The analysis of initial stiffnesses presented above shows that the stiffness ratio depends on many factors. To aid in the risk assessment of shear wall structures in nuclear facilities, it is recommended to: (1) base flexural stiffnesses on cracked section properties, (2) include shear flexibilities, appropriate effective shear areas and shear lag effects, and (3) apply a further reduction factor to the stiffnesses of 0.90 (COV = 0.07)

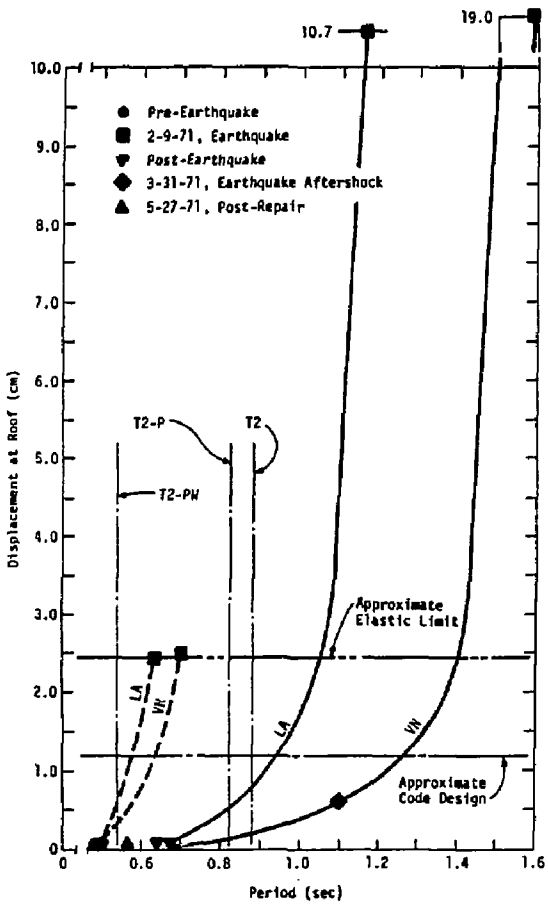

Fig. 2-8 Peak Response Observations, Transverse Direction for the Holiday Inn Orion (V.N.) and Holiday Inn Marengo (L.A.) Buildings

for flexure and 0.80 (COV = 0.12) for shear. These numbers recognize the detrimental effects of microshocks prior to the critical portions of the earthquake.

These recommendations are based on the consideration of the fact that shear walls in nuclear facilities are very heavy, and the penetration of shrinkage strains is limited. On the other hand, the vertical restraint is severe because of stiff columns. For example in the Zion plant the large steel columns and steel bracings restrain the shrinkage and partially support the weight of upper stories. Furthermore, the strength of concrete is relatively high, typically greater than 6000 psi, which means somewhat higher shrinkage effects. For lack of reliable data, the above considerations are judged to cancel out and justify the recommended values.

It is necessary, of course, to examine the effects of these uncertainties in initial stiffness on the response. Fortunately, the frequencies of these wall structures fall in the acceleration region of the NRC spectra and of the ductility-based spectra. Above about 2 cps the acceleration is not sensitive to a change in frequency. For example a change of frequency from 10 cps to 5 cps results in a change of acceleration of about 10 to 20% depending on the ground motion maxima. Between about 2 cps and 8 cps the acceleration is constant. This uncertainty is much less than the effects of special characteristics of the input.

The large reduction of stiffnesses of walls can change the torsional properties of the structure, depending on the location of the critical walls. In fact, for a uniform design which considered torsion, the walls on the perimeter would be stressed highest and their loss of stiffness could shift the center of stiffness appreciably and influence subsequent behavior. A static nonlinear analysis would shed light on this problem.

2.6 Behavior of Low Shear Walls

Inasmuch as low shear walls dominate reinforced concrete structures in nuclear facilities, they receive particular attention in this study. The evaluation is hampered by two facts; first, most investigations have been design (lower-bound) oriented and therefore have been primarily concerned with means to create safe structures. Second, the vast majority of tests and therefore the associated thinking or explanations were for walls in which flexure governed behavior.

Slenderness of walls is commonly measured by the h_w/l_w ratio, where h_w and l_w are the height and length (width, depth) of the wall. Walls with a ratio less than unity are low (short, squat), whereas ratios greater than 2 define tall or slender walls. Walls with $1 < h_w/l_w < 2$ are in the transition region but unusually behave more like low walls; in these diagonal tension and flexure are both significant. Most tests were performed on single-panel (one-story and one-bay) walls for which h_w and l_w are evident. It is less obvious what the height and length are for a wall with several stories or bays. Multibay continuous walls are rare in typical buildings but are common in nuclear facilities. For example, the wall between the auxiliary and turbine buildings of the Zion plant is 108' high with five stories and 266' long with 12 bays. If there is strong interaction between the walls and the frame, h_w and l_w may probably be taken as the overall dimensions. Then floors, beams and columns act as web reinforcement. For taller structures the differences of deformed shape between walls and the frame are more pronounced and h_w/l_w tends to lose its significance.

Actually, the moment-to-shear ratio or M/Vl_w is a better parameter distinguishing flexural and shear behavior. This is especially true in multistory structures loaded at several levels. The inelastic M/V ratio is required which can result in higher shears than an elastic analysis for a given flexural capacity.

When flexure is critical in taller walls, (1) horizontal cracks develop which lead to increased deformations and perhaps to sliding shear; (2) vertical edge members and vertical steel near the boundaries are important; (3) deformations, ductility, and hysteretic energy absorption can be high; and (4) increased flexibility means lower spectral accelerations. Study of research results and their discussions must keep these attributes in mind.

In contrast, in low walls shear often controls, flexure has little meaning, plane sections do not remain plane, drift is smaller, and higher forces are generated. It is convenient to classify shear stresses as low (less than 3 $\sqrt{f_c'}$) and high (greater than 7 $\sqrt{f_c'}$); low stresses normally do not cause problems in well detailed walls.

As mentioned previously, shear deformations may constitute a significant portion of the total deformations. Fig. 2-9 shows a plot of ratios of shear deformations to total deformations for walls, as a function of the moment to shear ratio (Ref. 49). The large experimental scatter in shear stresses is evident from Fig. 2-10 (Ref. 40) where many wall tests, tall and short, are plotted against the concrete strength. In most of these tests the concrete strength was rather low.

It is instructive and necessary to review the failure modes of relatively low walls: flexure (yielding of vertical steel followed by steel fracture, concrete crushing, or steel buckling); diagonal crushing (between diagonal tension cracks); diagonal tension (steel yielding and fracture at diagonal cracks); and sliding shear (loss of interface shear transfer strength across horizontal cracks). Other failure modes are: deterioration of connections between the wall and boundary elements, failure of boundary elements, and buckling of the wall. All of these failure modes have been observed and the relevant types are examined in the following.

Even in short walls flexure can play a deciding role. If horizontal cracks are opened by the cyclic moment, sliding shear usually occurs along horizontal cracks. This is likely in the 3 $\sqrt{f_c'}$ to 7 $\sqrt{f_c'}$ stress

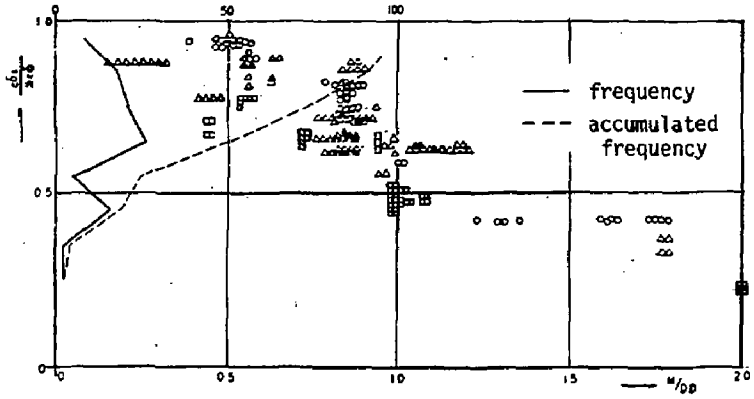

Fig. 2-9 Shear Deformations as a Fraction of Total Deformations versus Moment/Shear Ratio

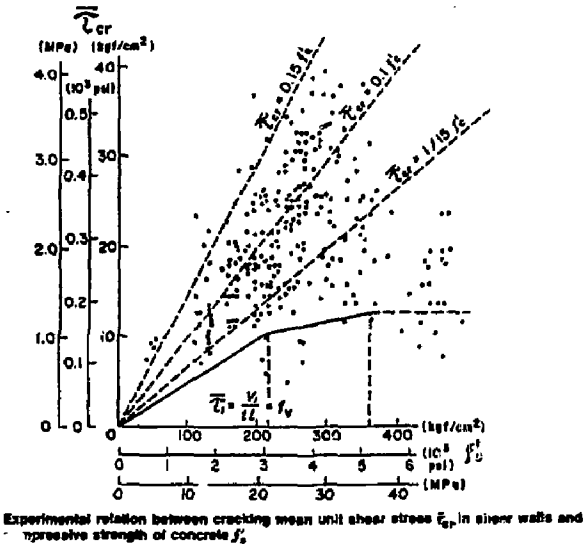

Fig. 2-10 Measured Shear Stresses at Cracking in Walls

range (Ref. 30). Resistance to sliding shear is provided by aggregate interlock (shear friction), dowel action of vertical steel or columns, and diagonal steel, if present. The level of shear strength is $A_v f_y \mu \leq 0.2 f_c' A_c$ or $800 A_c$ lbs, where $\mu = 1.4$ except $\mu = 1$ at construction joints and A_v is the area of vertical steel. Cycling reduces strength by about 15% but stiffness can deteriorate much faster (Ref. 31) and lead to significant loss of hysteretic absorption. The hysteresis curve is pinched and contains a segment with very low stiffness (Fig. 2-3a). The possibility of high ductility ratio is meaningless in this case.

For conditions typical in a nuclear facility, the estimated sliding shear capacity is $V_u = \rho f_y = 0.003\ (60{,}000) = 180$ psi, but not more than $0.2\ (6600) = 1320$ psi or 800 psi. Thus the strength is 180 psi or about $2.2\sqrt{f_c'}$ for 6600 psi concrete. These calculations are for only the wall; column steel, notably the steel columns of the Zion plant, would add significantly to the sliding shear strength. If the columns are included, the steel ratio would be about twice the above value. It is likely that steel columns would provide enough dowel capacity to prevent sliding shear failures (see Chapter 3).

In very low walls flexure and consequent vertical yielding play a negligible role. Diagonal cracks form in two directions, rather than horizontal flexural cracks. Diagonal compressive forces act between the cracks and a truss mechanism develops in which shear reinforcement and boundary elements are the remaining elements.

A free body bounded by diagonal cracks is shown in Fig. 2-11. It is clear that both vertical and horizontal wall steel are important. The wall steel must be well anchored at boundaries. The compressive stresses in the panel may be viewed as a "diagonal compression field" (Ref. 32). Failure can be either by general yielding, which is easily calculated, or by compressive crushing. It should be noted that the compression field intersects the columns and beams of low walls, which underlines the importance of wall-frame

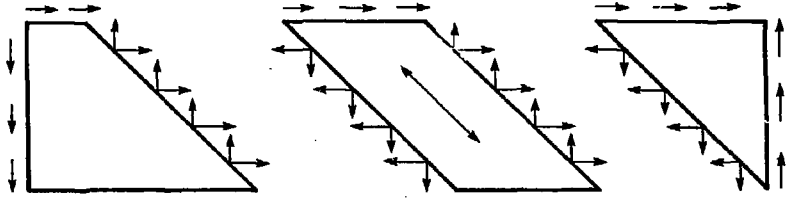

Fig. 2-11 Free Body of Wall with Diagonal Tension Cracks

interaction. The top beams must have sufficient stiffness to resist the forces. The inclination of the struts depends on relative stiffnesses of wall, beams, and columns and ranges from 30^0 to 60^0.

The crushing strength is significantly reduced by transverse diagonal tension to as low as 0.2 f_c'. The reduction depends on the shear strain γ_m (diameter of the strain circle) and ε_0 (strain at peak cylinder stress of concrete) as shown in Fig. 2-12 (Ref. 32). Thus wall deformations, (flexural and shear) decrease the diagonal compression capacity.

For a 45^0 truss, equilibrium gives a crushing shear stress

$$v_{cr} = 0.5\, k f_c' \tag{2-11}$$

where k is the effective strength factor.

An evaluation of k in this equation from 14 PCA tests, in most of which flexure was significant, resulted in an average value of k = 0.25 with COV = 0.32. For negligible axial force and neglecting flexural distortions, shear distortion can be related to story drift r by the empirical relationship $\gamma = 0.76r$, where r is the relative story displacement divided by the story height (Ref. 33). Using $\varepsilon_0 = 0.0025$ and the equation in Fig. 2-12, one obtains

$$k = \frac{3.6}{1 + \frac{2(0.76r)}{0.0025}} = \frac{3.6}{1 + 600r}. \tag{2-12}$$

The measured drifts at failure in 11 unrepaired PCA walls averaged r = 3.0% with COV = 0.20. However, in these tests flexural deformations were important. The shear distortions averaged r = 1.96% with COV = 0.30 for all 14 (unrepaired and 3 repaired) walls.

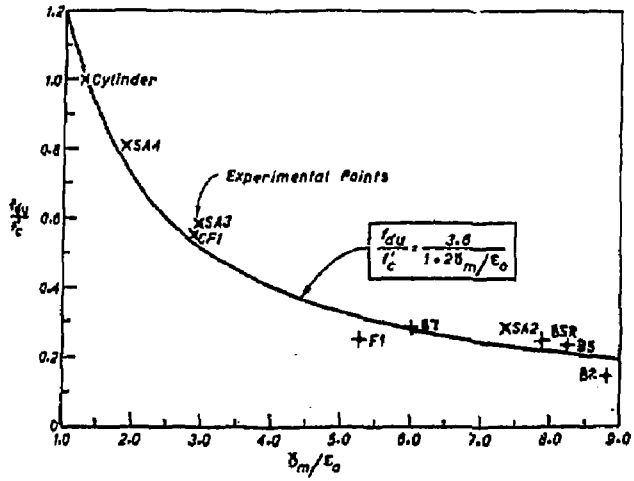

Fig. 2-12 Principal Compressive Stress at Failure as a Function of Shear Strain

Considering drifts observed in low wall tests in which flexural yield was not reached (see Chapter 4), a lower value of r = 1.0% is recommended. Then k = 0.51 and

$$v_{cr} = 0.25\ f_c' \tag{2-13}$$

is the shear stress in low walls at diagonal crushing with COV = 0.30.

It has been advocated in New Zealand that only the steel should be relied upon in low walls. However, analysis of test data does not support that excessively conservative view. Only after cyclic flexural yielding, which produces an open horizontal crack, is the concrete contribution lost in walls without stiff vertical boundary members which delay sliding.

Preoccupation with tall walls in research, thinking, and design is illustrated by the fact that code equations specify only the amount of horizontal shear reinforcement $\rho_h f_y$. Yet horizontal steel becomes less effective as h_w/l_w decreases and vertical reinforcement becomes important. At the end however, equal amounts of horizontal and vertical steel ratios are used.

The contributions of vertical and horizontal steels were separated in the SSMRP analysis (Ref. 2). The ultimate shear stress is

$$v_u = v_{cu} + v_{su} \tag{2-14}$$

$$v_{cu} = 8.3\ \sqrt{f_c'} - 3.4\ \sqrt{f_c'}\ (\alpha - 1/2) + \frac{N}{4\ell_w h_w} \tag{2-15}$$

$$v_{su} = A\rho_v f_y + B\rho_n f_y \tag{2-16}$$

where

N = the vertical compression,
ρ_v = vertical steel percentage,
ρ_h = horizontal steel percentage,
$\alpha = h_w/l_w$,
$A = 1$, $B = 0$ for $\alpha < 1/2$,
$A = 0$, $B = 1$ for $\alpha > 1$.

The coefficient A decreases linearly and B increases linearly between $\alpha = 1/2$ and $\alpha = 1$. This equation permits an improved estimate of the shear capacity of a given wall. Actually, both types of reinforcement are still effective somewhat outside the given limits, but the numbers are not sensitive as long as both kinds of steel are used. The equation reduces to a previously published one for equal amounts of vertical and horizontal reinforcement, since $A + B = 1$. Typically, the concrete contribution is about three times the steel contribution, thus the sum is less sensitive to A and B. It is noted here that several typographical errors are on pages 3-7 and 3-8 of Ref. 2, including two in Equation 3-6.

The shear area used to convert stresses to forces is often taken as h.d, where h is the wall thickness and d is the effective depth. The ACI Building Code and most US research reports assume $d = 0.8l_w$, but often take d as the total depth of the wall. Actually, d depends on the size of columns and the amount of reinforcement in the boundary columns. In any case, these differences should be recognized when evaluating and comparing test data.

In some of the tests in Ref. 25 vertical local N was applied, which adds $N/4h_w l_w$ to the strength. This was added in both formulas. Also, it has been recommended (Ref. 17) to ignore the concrete cover when evaluating the diagonal crushing strength (for example using Eq. 2-13); this was not done in these calculations.

Several tests were not considered because premature failure occurred (for example, due to slip between the wall and the frame in two tests at the University of Michigan) or excessive strength was contributed by unusually

heavy frames (Benjamin's tests at Stanford). A prediction equation cannot work for very unusual cases. The two walls from Ref. 37 failed by sliding shear after flexural yielding; these did not have strong edge columns to act as dowels. The seven walls from Ref. 36 were not low if the total 3-story height is considered; the total height was used in Eq. 2-14, for all walls.

Which of the three equations should be used in a best-estimate calculation? The shear-friction equation $\rho_v f_y$ is actually part of Eq. 2-14 if the concrete contribution is ignored. Sliding shear may be a problem only if cyclic flexural yielding occurs and the vertical edge members have little dowel capacity. It is recommended that this failure mode be discounted in the analysis of the massive shear walls of nuclear facilities, *as long as vertical tension due to pressurization is not present.*

The two other equations serve different purposes. Equation 2-13 predicts diagonal crushing strength in low walls but does not consider the slenderness. Equation 2-14 is equally good in estimating shear strength and reflects the effect of h_w/l_w and the steel.

It is proposed that both Equations 2-13 and 2-14 be used in shear capacity estimation. Using the lower predicted values in each of the 32 tests (PCA, Japan and Berkeley), the result is

$$\text{average } \frac{\text{predicted}}{\text{measured}} = 0.99,$$

$$\text{COV} = 0.26.$$

This is an excellent correlation considering the diversity of tests. Of the 32 numbers, Eq. 2-13 controlled in 9 cases.

This data base is much wider than used previously in developing equations. It should be noted, however, that special failure modes, such as sliding at interfaces, fracture at openings, or wall instability are not and

cannot be covered by such equations. The safety of complex structures and the discovery of special failure modes will have to be the task of experts. A detailed comparison of failure modes with prediction might be interesting but this has not been done.

It appears that shear lag effects in box sections may alter the stress distribution sufficiently to lower shear stiffness and strength (this factor was discussed previously). Several box and cylinder specimens were tested in Japan (Ref. 24). The two box sections that failed in shear had predicted/measured ratios 1.67 and 1.92 by Eq. 2-13, and 2.96 and 2.13 by Eq. 2-14. These are much higher than the highest in the 32 wall tests analyzed above.

This section was restricted to the prediction of the shear strength of low walls. It will be claimed in Chapter 4 that deformations (drift) must also be limited to avoid excessive damage.

2.7 Summary

Several key aspects of the SSMRP fragility analysis were evaluated in this chapter. They relate to the ductility-based reduction of the response, the associated damping values to be used, the initial stiffness of shear walls, and the capacity of walls.

The uncertainties inherent in the ductility-based spectra are well known, but additional questions specific to concrete structures in nuclear facilities were raised. These relate to the shape of the hysteresis curves and the recommended ductility values. A reduced damping ratio was indicated which does not account for hysteretic energy absorption.

The low measured initial stiffness of walls, often as low as 20% of the predicted values, was analyzed, explained, and evaluated.

An extensive study of an extended pool of data resulted in an improved procedure for the estimation of shear failures of low walls that are ubiquitous in nuclear plants.

3 FRAGILITY ANALYSIS OF THE ZION PLANT

3.1 Introduction

The fragility analysis method within the SSMRP was evaluated in Chapter 2 as a general approach. The principal assumptions were examined, together with the variability of material properties and shear wall behavior in the light of recent information.

This chapter is devoted to the study and assessment of the application of the fragility analysis to the Zion plant. The primary sources of information were References 2 and 38. Although this discussion is plant-specific, some of the conclusions are applicable to other nuclear facilities.

As in Chapter 2, special attention is paid to low shear wall behavior. In addition credible roof failures are considered.

3.2 Main Features

The fragility parameter, that is the horizontal axis of the fragility plots, was in most instances selected to be the acceleration at Node 3006 of the auxiliary building at elevation 642 feet, near the roof. This acceleration was calculated by time-history analyses for 30 simulated motions in each of six ground acceleration intervals. The stresses in critical elements of the attached buildings were tied to this acceleration from a subset of the analyses.

Linear analysis was used in the structure response analysis but soil-structure interaction and torsion were considered. Significant torsion exists for N-S excitation (see Fig. 3-1). Nonlinearity was included in a simplified manner: ductility-based response deamplification was used to reduce element stresses. The success of this approach hinges on the development of nonlinearities throughout the structure at a uniform rate.

Local nonlinearities, even if present, are not allowed to influence at a different rate the overall response.

Most simplified analysis and design methods rely on similar assumptions that work for optimally-proportioned structures. It is doubtful that many three-dimensional buildings satisfy such criteria; in fact, a good seismic design should strive for the opposite: sequential and progressive failure of load-sharing systems.

Nonstructural block walls were not included in the idealization. However, these 12 in. walls, present throughout the auxiliary-turbine building complex, alter the stiffness characteristics. In particular, they affect torsional response in the elastic range and much more so as they fail progressively. An estimate of this effect can be made without great difficulties (see Chapter 5).

The failures of the weakest critical elements (walls, roofs) were analyzed independently. The effect of partial failure of a primary wall on the response of other elements could be important. Ignoring the interaction is on the safe side if there is no overlap of the fragility curves and the failures are of similar importance; otherwise, the sequence of failures remains uncertain. A static, nonlinear analysis would be helpful. Another question arises for very stiff structures because the response can increase as stiffness is diminishing.

As explained in Section 2.6, the response of walls is strongly influenced by vertical forces. Pressure in the concrete buildings (aside from the containment) was not considered possible in this plant. However, in some plants room pressure can develop and cause tension in walls; the shear stiffness is drastically reduced by tension.

The failure of wall anchors prior to wall collapse was not studied in the SSMRP though critical equipment might be attached to walls. A preliminary examination of this problem is included in Section 3.7.

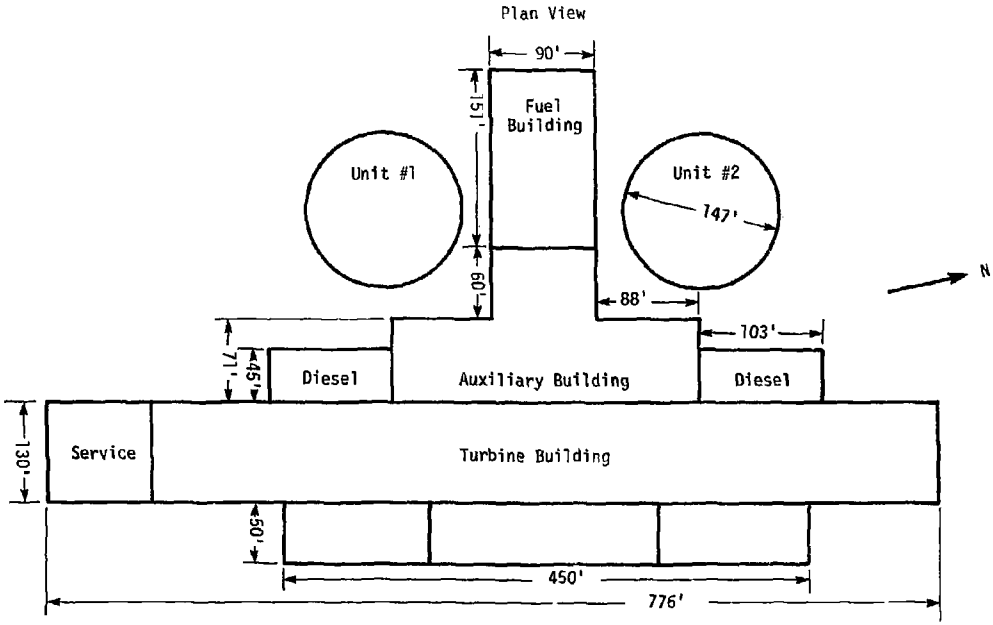

Fig. 3-1 Zion Station Plan View

3.3 The Main Wall

One of the critical structural components of the Zion plant is the large common shear wall between the auxiliary and turbine buildings (Fig. 3-1). The wall is sketched in Fig. 3-2. A steel frame with tubular diagonal bracing in four bays per floor is embedded in the wall.

As it is explained in Section 2.6, two important factors governing the behavior of shear walls are the interaction with the frame and the moment/shear ratio (or height-to-width ratio). The roles of these factors are not evident in the present case. If the interaction is reliable, the entire wall may act as a unit and the h_w/l_w ratio is taken for the whole wall. This is possible only if compression and tension forces can be transmitted across steel members and between the wall and the outside boundary frame. Truss action depends on the ability of the boundary frame to take the tensile or compressive forces (Section 2.6). The steel columns act as stiff dowels that are expected to prevent sliding shear failures. On the other hand, the steel frame provides stiff restraint and promotes shrinkage cracking.

The compression field is accompanied by inclined forces acting on the frame. At the very top the beams must be stiff enough to supply the reaction; fortunately, the shear and diagonal forces are small at the top. The interior beams and columns receive forces from both sides and these forces partially cancel out. The tension between the end columns and the end panels must be transmitted by positive connections, such as anchor bolts, and the wall reinforcement must be anchored to develop the tension; otherwise a failure plane develops along the end columns or at the anchor bolts. There is no empirical information or design guides to help in the estimation of the interface forces; conservatively, the forces are taken at the yield level of the wall reinforcement.

The fragility analysis in Ref. 2 hinges on the shear capacity of the studs welded to the column webs between elevations 592 ft and 617 ft. The forces in the studs were calculated from the shear flow equation VQ/I for the entire

A #6 @ 12 0.306%

B #7 @ 12 (each face) 0.418%

h = 24"

f'_c = 6.1 ksi

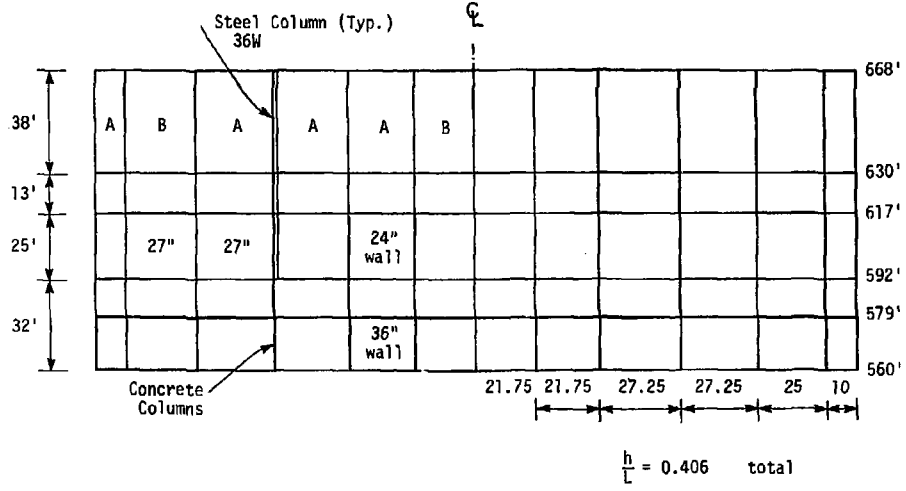

Fig. 3-2 Elevation of Main Shear Wall

width of the wall. However, the wall is not slender and plane sections do not remain plane; thus flexural equations such as VQ/I do not apply. The shear stresses from the floor inertia forces are nearly uniform rather than parabolic along horizontal sections; the uniform stress is 2/3 of the parabolic value.

The second question regarding the fragility analysis of the main wall concerns the failure mode of the studs. In Ref. 2 it was assumed that welded studs fail in a brittle manner at a shear force,

$$930\, d^2 \sqrt{f_c'} \quad \text{(lbs)}, \tag{3-1}$$

where d is the diameter of the stud, in this case 3/4 in. Therefore, the story shear force-drift curve shows a sudden loss of strength when the studs fail suddenly and nearly simultaneously, as shown in Fig. 3-3. It is assumed that after stud failure no interaction remains between the columns and the wall. The concrete panels between columns subsequently act as cantilevers and their capacity is limited by flexure at a low load (Fig. 3-3).

It is questionable that stud failure is brittle. There are shrinkage cracks at each stud, and a gradual loss of stiffness as the concrete around the studs deteriorates and a failure cone forms after considerable slip. The studs themselves are not likely to fail before large deformations; this is indicated by the fact that the capacity does not depend on the strength of the stud material.

The studs are not loaded as long as a perfect bond exists between the surfaces, and they become effective only as slip develops. Short studs fail by pullout; intermediate length ones by a cone formation and pullout; and long studs fail by concrete crushing and eventually by weld fracture. The 6-in. studs in the Zion wall are long. Such long studs undergo significant bending, even into double curvature, before failure. Moreover, the strength does not increase much beyond a stud length of about four diameters.

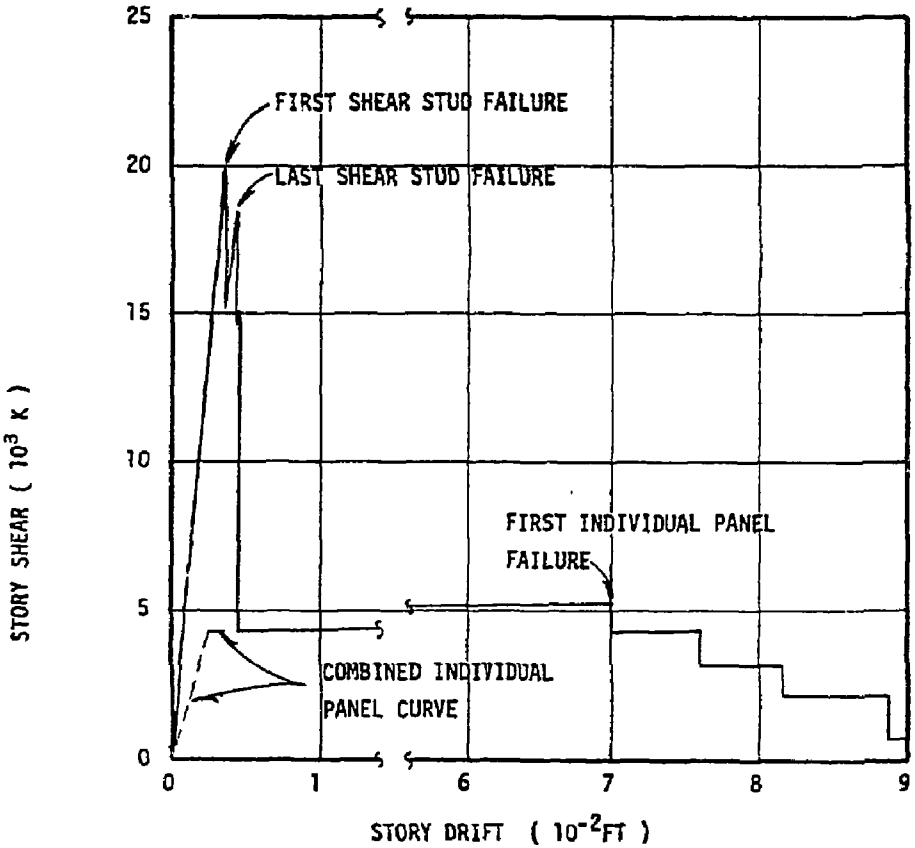

Fig. 3-3 Story-Shear versus Drift (Ref. 2)

Most of the available information on stud behavior was developed for use in composite construction. Design codes, based on test results in the 1950's, assume that studs along beams and embedded in concrete slabs share the load equally. Since the shear force and shear flow usually vary linearly along beams, considerable redistribution is recognized. This approach was used even before other ultimate strength concepts were widely adopted. In the present case gradual loss of stiffness of the studs loaded nearly uniformly along the column led to a nonlinear force-drift relationship.

Several force-slip curves are shown in Fig. 3-4 (Ref. 39). It is seen that large scatter exists and considerable slip and loss of stiffness occurs. The following equation is proposed to approximate the curves

$$V = 40\ (1-e^{-40s}). \tag{3-2}$$

This is an extrapolation to higher shear values for the 6-in.-long studs used in the wall.

To permit a nonlinear analysis of the wall-frame system, the stiffness is required:

$$k = \frac{dV}{ds} = 1600e^{-40s} \tag{3-3}$$

Each stud has a tributary area of 12 x 12 in., and therefore the interface shear stiffness is

$$k_i = \frac{dV}{ds} = 11e^{-40s}\ \frac{ksi}{in}. \tag{3-4}$$

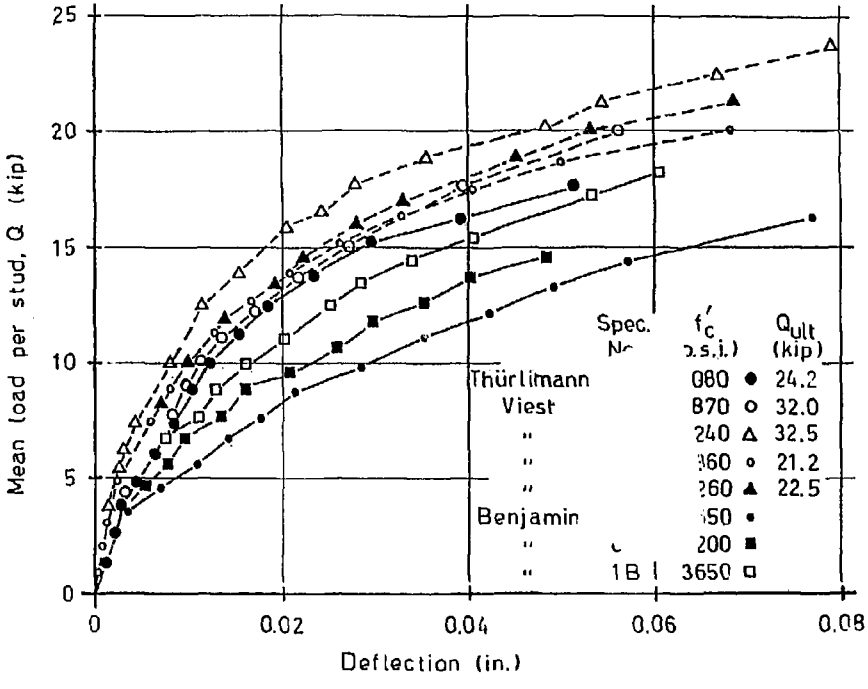

Fig. 3-4a Shear Load-Deflection Curves for 3/4 in. Dia. x 4 in. Studs (Ref. 39)

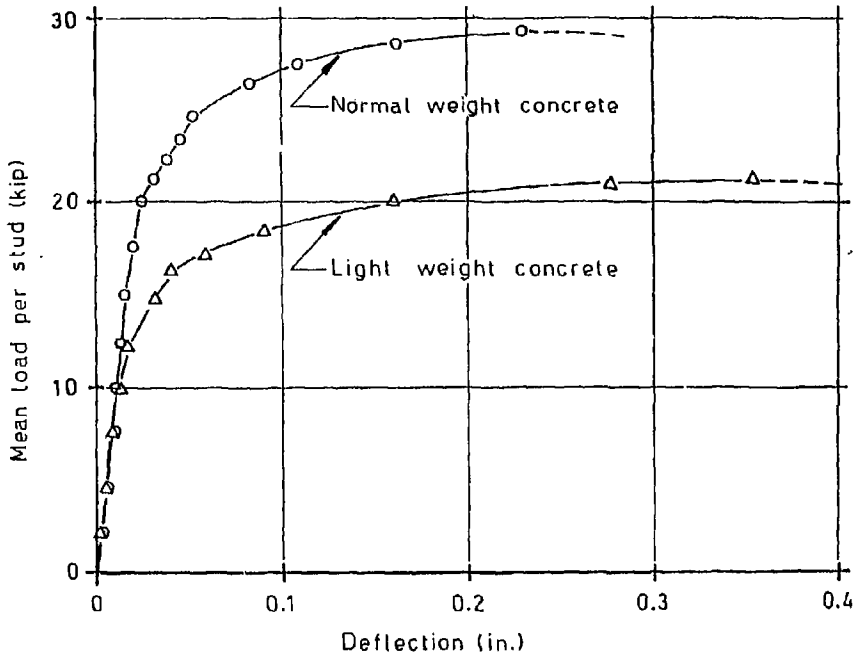

Fig. 3-4b Load-Deflection Curves to Ultimate for 3/4 in. Dia. x 4 in. Studs (Ref. 39)

This can be used in a finite-element program to predict the response of the wall.

Since there is large variation in the data, the various panels subjected to a nearly equal shear stress will not respond identically. This fact introduces another cause of gradual loss of overall stiffness.

A preliminary analysis of the simple model of Fig. 3-5a was performed at Cornell University using a nonlinear finite element analysis with interface elements and graphic output. The purpose of this crude analysis was only to get a rough idea of nonlinearity for the wall dimensions, force levels, and stud properties given. The deformed shape and load-displacement curve are shown in Figs. 3-5b and 3-5c. The nonlinearity is not great for this set of properties.

The effect of 10 load cycles at three load levels is shown in Fig. 3-6a (Ref. 40). Level B was about half the monotonic strength, and a serious loss of stiffness is evident. The secant stiffness after 10 cycles at level B was half the initial stiffness. The effect of few high-level cycles on strength is not reported. Another cyclic load-slip curve for studs attached to steel angles is shown in Fig. 3-6b from Ref. 41. Although the loading of angles is somewhat different, the large deterioration and pinching is evident. Deflections at failure were as high as 24 times the elastic deflections.

Reference 40 gives the capacity as

$$V_u = 0.5\, A_s \sqrt{f_c' E_c}, \qquad (3\text{-}5)$$

where A_s is the area of the stud.

For f_c' = 6600 psi and d = 0.75 in. Eq. 3-1 gives 42.5k and Eq. 3-5 results in 38.6k.

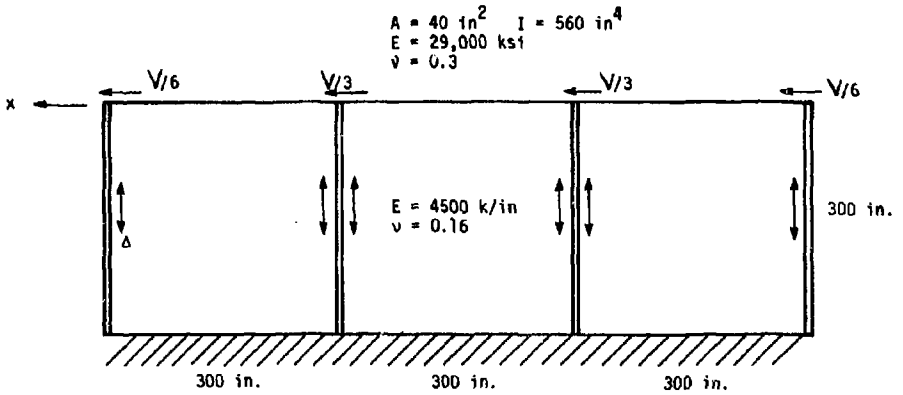

t = 24 in.

Shear-slip between columns and walls:

stiffness $k = 11e^{-40\Delta}$ $\frac{ksi}{in}$

or approx. $k = 1 - 33.7\Delta + 310\Delta^2$

Fig. 3-5a Input Data for Wall Analysis

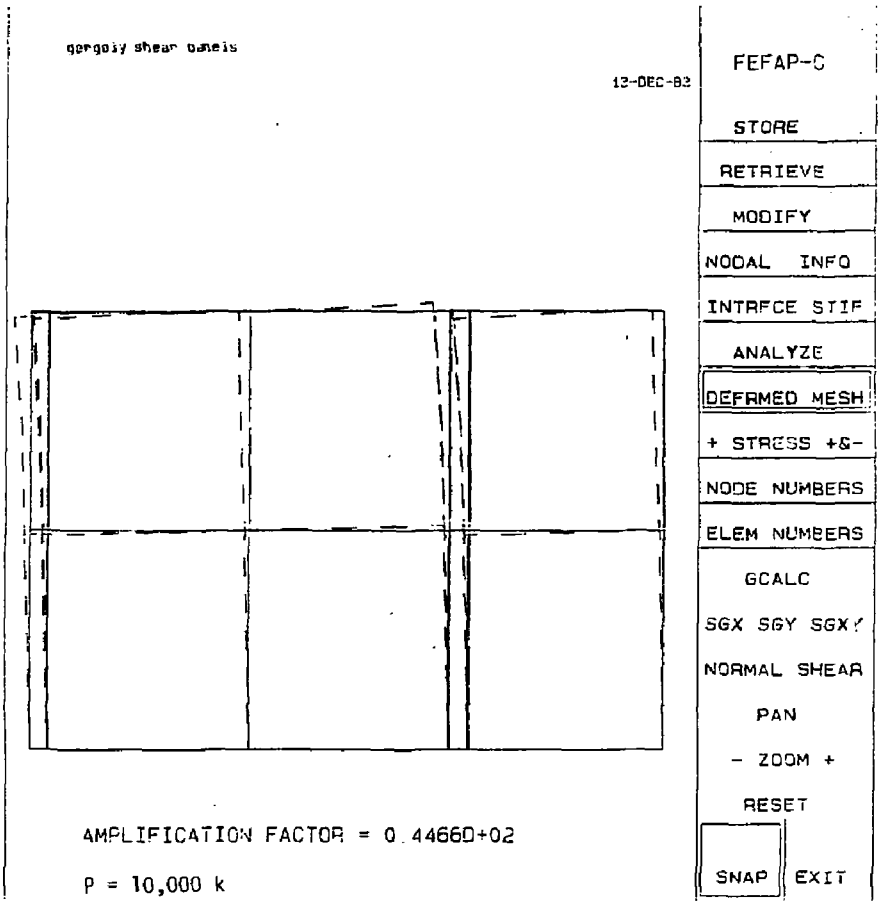

Fig. 3-5b Deformed Wall

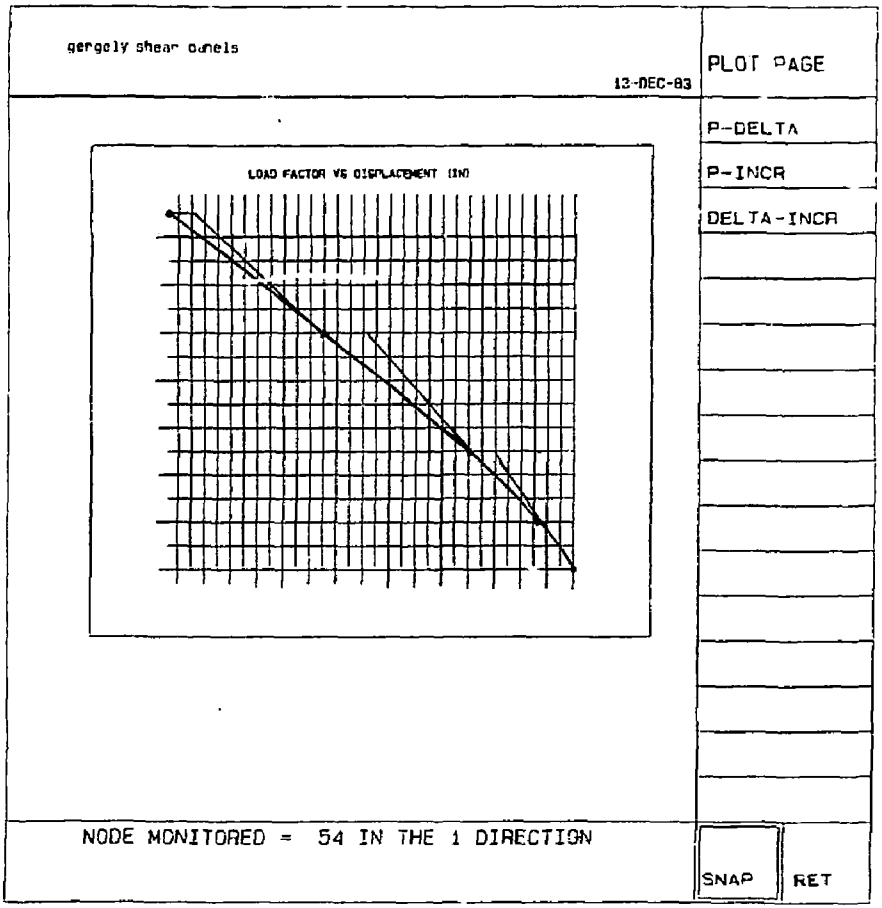

Fig. 3-5c Preliminary Nonlinear Analysis of the N-S Common Wall with Studs

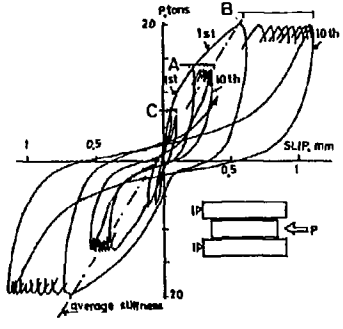

(a)

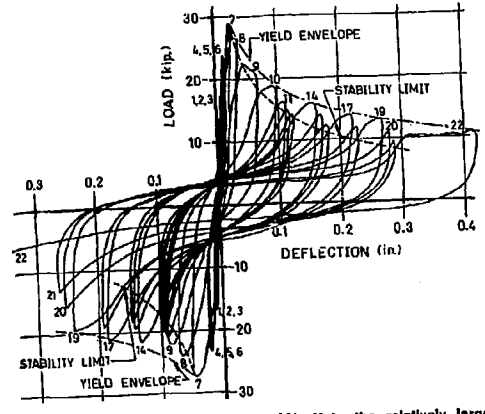

Load-deflection loops (Connection A3). Note the relatively large deflections reached before failure.

(b)

Fig. 3-6 Shear Studs with Cyclic Loading

To obtain an estimate of the shear in a stud at the peak story shear of 20k (Fig. 3-3), a uniform shear stress is assumed. Then

$$v = \frac{20{,}000}{246(12)(24)} = 280 \text{ psi.}$$

For a tributary area of 12 x 12 in., the shear force is 40.7 k. The slip is about 0.06 in. at v = 250 psi.

It is important and instructive to compare the estimated strengths and stiffnesses of the wall elements. The concrete stiffness is shown in Fig. 3-7 for G/2 and G/5. The strength levels are noted at $2\sqrt{f_c'}$ when cracking is noticeable and at $4\sqrt{f_c'}$ (diagonal cracking). Drifts of 0.04% and 0.2% denote initial cracking and extensive cracking, respectively. The total stiffness and yield strength of the 6 diagonal braces are shown for an assumed 0.5-in. tube-wall thickness and 50 ksi yield.

Two additonal observations need to be made. As it was shown in Section 2.6, the initial wall stiffness is a strong function of shrinkage strains. The steel frame, with the studs and diagonals, provides an unusually large restraint and therefore shrinkage cracks should be common. Also, the gradual loss of stiffness and consequent hysteresis will introduce appreciable energy dissipation that must be evaluated from tests.

The main conclusion of this analysis is that the transition from the shear wall to individual flexural cantilevers will be gradual. Significant shear transfer between the panels and the columns will be maintained. Therefore, the stiffness and the strength of the wall will remain much higher than that of the separate cantilevers. A relatively simple two-dimensional nonlinear analysis can shed light on the force transfer process.

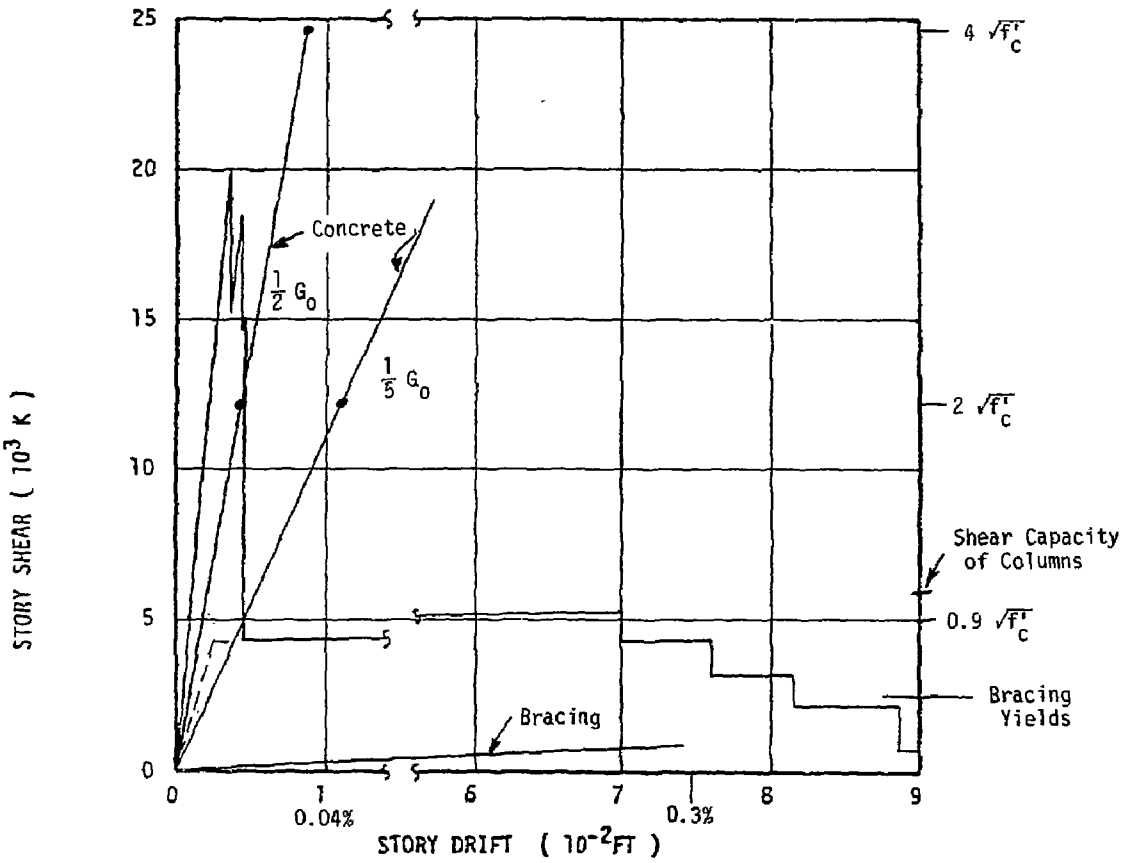

Fig. 3-7 Force-Deflection Curve for Common Wall Between Els. 592' and 617'

With the gradual stiffness reduction and the larger strength of this wall, it is likely that other walls, especially at lower elevation, will become critical. Most of those walls do not have studs.

If shear controls the strength, as it was claimed in the previous discussions, the lowest of the following control the story shear:

(1) Equation 2-14, v_u = 935 psi but limited to 10 $\sqrt{f_c'}$ = 810 psi.

(2) Equation 2-13, v_u = 1650 psi.

(3) Drift of 0.4%. At a conservative $G_o/10$ the corresponding stress for such a strong wall can be estimated to be 1850 psi. However, this limit should normally be checked using displacement calculations.

As mentioned earlier, sliding shear failure will be prevented by the stiff steel column.

Taking the lowest value of 810 psi, the corresponding wall shear is 62,000 k which is much larger than the values postulated in Fig. 3-7. This example indicates how widely different numbers result from different assumptions or judgmental considerations, even without consideration of nonlinearities. Extensive studies or input from experts are often dispensable.

Eq. 2-13 was derived from the compression field theory and assumes that the entire field can be developed. If that is not the case, compression struts will act corner-to-corner in each panel of the steel frame. The approximate forces are $V = 12(0.2\ hf_cL/12)\ 0.707 = 0.14Lhf_c = 10{,}800\ f_c$. If one takes a relatively high effective strength value $f_c = 2\ f_c'/3$ because the distortions are small, V = 47,500 k results. The corresponding tension in the columns is (47,500/12) 0.707 = 2800 k, and part of the strut force produces shear in the columns.

The importance of wall-frame interaction becomes clear upon examination of the rightmost free body in Fig. 2-11, which is the end of the wall. If h_w is the height of the wall and the crack is at 45^o, the total shear force acting on top of this element is h_wV/L, where L is the total length. Equilibrium at yield demands

$$\rho h_w h f_y = h_w V/L$$

where ρ_h is the horizontal steel percentage and h is the wall thickness.

Therefore

$$V = Lh\rho_h f_y = A_w \rho_h f_y$$

where A_w is the horizontal wall area. In the present case,

$$V = 266(12)(24)(0.0034)60 = 15{,}630 \text{ k.}$$

It is interesting to note that this is the same as the steel contribution in Eq. 3-14 for equal vertical and horizontal steel; these numbers ignore the contribution of concrete. The value is also equal to the shear friction limit for a coefficient of friction of unity. The capacity of end columns to provide support to the diagonal struts is not considered.

3.4 Other Walls

Several other walls in the E-W and N-S directions of the building complex were analyzed in Ref. 2. It was claimed therein that failure of the selected walls, including the main wall discussed in the previous section, can be evaluated independently, and failure of any of these walls will lead to immediate failure of the other walls.

Although this deliberate disregard of redundancy and load redistribution substantially simplifies failure analysis and is on the safe side as far as

design goes, it does not allow a realistic risk assessment. Nonlinear behavior and loss of stiffness of these walls introduces load sharing, especially for dynamic loading, that should lead to a higher capacity.

The consideration of load sharing and redistribution is especially important because the E-W diesel generator room walls are expected to fail at nearly the same load level as the main wall discussed previously. It is admitted that the nonlinear interaction through torsion is complex, but a static nonlinear analysis would reveal the extent of load transfer. It would also help to assess the value of system ductility much more reliably than simply reducing the local ductility.

There are several E-W walls in the diesel generator building and it is unlikely, given the variations in capacities and the uncertainties of nonlinear torsional effects, that the failure will be sudden. Redistribution of forces would take place, and therefore the fragility curves are expected to be flatter than those shown in Fig. 3-8.

The significant loss of lateral stiffness of the buildings as walls crack leads to much higher displacements, especially in such stiff structures. The increased displacements are important because there is only a 1-in. gap between the auxiliary-fuel handling buildings and the containment, though the soil flexibility is probably the most significant source of displacements.

3.5 Roofs and Floors

Several credible failure modes of horizontal diaphragms have been identified (Ref. 38). These include the failure of the roof bracing of the turbine building and the roof slab and truss of the auxiliary building. Considering the slenderness of the buildings, the large forces to be transmitted to the walls, and a lack of redundancy, these horizontal members should receive special attention.

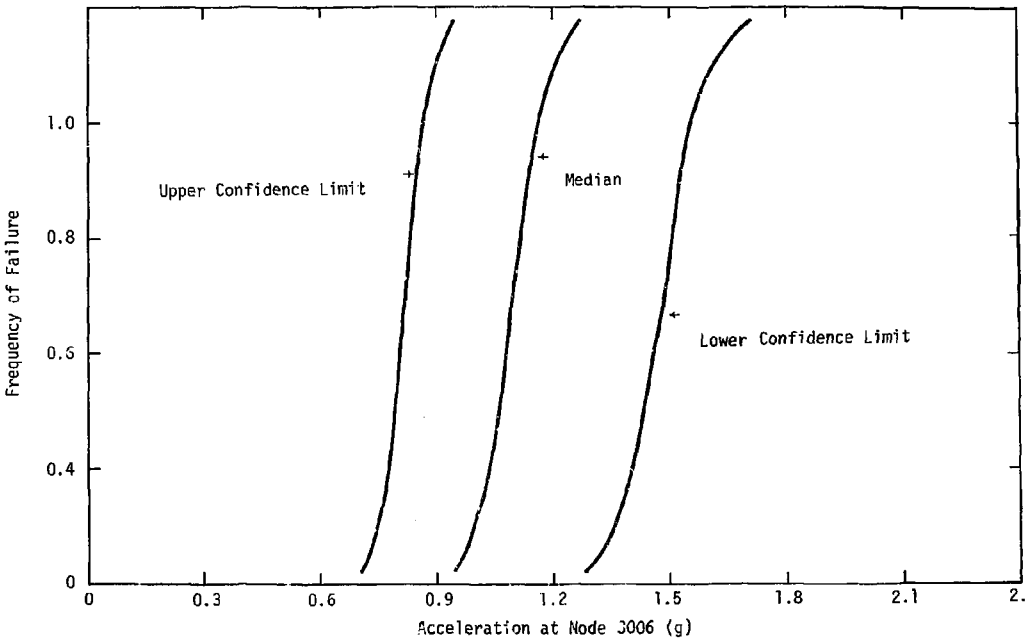

Fig. 3-8 Failure of Diesel Generator Building Walls

The roof of the pump enclosure room of the crib house is elongated in the N-S direction and fails due to E-W excitation. The method of capacity evaluation is not discussed in Ref. 2 but relatively little uncertainty is involved. The loss of stiffness leads to the out-of-plane failure of the N-S walls and the roof collapse.

The connection between the auxiliary building roof and the walls is a weak link. Its deterioration leads to out-of-plane wall bending failure and roof collapse. The calculated mean acceleration capacity at node 3006 is about 3.0 g based on linear response. The stiffness reduction of walls can lead to a lower capacity but the evaluation of this behavior sequence would require nonlinear analysis.

The pump enclosure roof has numerous large openings which are especially consequential in an elongated diaphragm affected by deformations. Not much is known about the effect of random holes in diaphragms. An elastic finite element analysis can easily predict stresses, but inelastic behavior or failure is a much more complex problem. More work is recommended in this area.

3.6 Containment Vessel

The failure modes of the cylindrical containment are strongly affected by the internal pressure and the level of tension in the wall. The shear stiffness and capacity are reduced as horizontal cracks form and remain open (Refs. 23 and 42).

Linear analysis of the vessel was used to perform the fragility analysis. However, the highly nonlinear shear behavior of cracked containments fundamentally alters the response (Refs. 43 and 44). Non-linearity reduces the stresses but increases displacements.

3.7 Anchor Failures

One of the critical local failure modes (limit states) in a nuclear facility is anchorage pullout of equipment or supports. For example,

equipment may be attached to walls and severe cracking of the walls can lead to anchorage failure.

This problem has not been analyzed in Ref. 2 and, in any case, little information is available. There are two questions: the critical damage state of the wall, and the force combinations necessary for pullout.

Based on the discussions presented in Section 2.6 and Chapter 4, a drift (shear distortion) level of 0.1% (0.001 radians) signifies extensive diagonal cracking in low walls. This criterion may be taken as a lower bound for wall damage.

It is more difficult to estimate the forces (shear, bending, tension) required to free a specific wall anchor. The code contains simple provisions for estimating the pullout force. Push (punching) tests on tensioned panels have shown little decrease of punching resistance with biaxial tension up to 0.9 f_y (Ref. 45). More research is required to evalute the anchor capacity in tensioned walls.

3.8 Summary

The application of fragility analysis techniques to the Zion plant were evaluated in this chapter. The failure of shear walls received particular attention. A different model of the failure mechanism of the N-S main wall was advanced.

It has become evident that there are no straightforward and foolproof methods of behavior and capacity prediction. An intimate knowledge and understanding of each type of material or structural element is a necessity. Since there is a large variety of elements and behavior is often controlled by details, the analysis requires great care and a coordinated effort by various experts.

4 OTHER APPROACHES

4.1 Introduction

The focal difficulty in seismic risk assessment, indeed in earthquake engineering generally, is the consideration of inelastic response. The most common analysis method, the ductility-based spectrum reduction, was used in the SSMRP and was evaluated in Chapter 2.

To circumvent the direct use of ductility factors, several alternatives have been proposed. It is not claimed here that they are clearly better, but they do offer additional insight into dynamic analysis and nonlinear behavior. Much more work is necessary, especially for high-frequency structures, before a choice can be made. Again, the goal of risk assessment is much more difficult than that of a safe design.

This chapter contains a brief review of some approaches that might be used to estimate inelastic response. The discussion is open-ended because many questions are still unanswered, especially for stiff structures not dominated by flexure.

4.2 Drift Criteria

The safety and response levels have historically been measured mainly by stress or force amplitudes. It has become increasingly clear over the past few years that distortions are equally important indicators of damage and most codes now have displacement limits.

Relative displacement may represent overall drift (relative to the base), interstory drift, or tangential interstory drift which excludes the rigid-body rotation of the lower floor. The interstory drift is used most commonly; for low structures without much overall flexure it is an acceptable substitute for the tangential interstory drift.

Drift is a reasonably good indicator of structural damage, the p-delta effect, and especially nonstructural damage. The limit is a function of the type of structure, the method of analysis, the lateral force level, the axial force level, and the influence of flexure.

As a clear illustration of the usefulness of drift limits is the fact that the ductility demand on very stiff structures is usually large, yet nonstructural elements are not extensively damaged at low drift values. Thus ductility is not a sufficient criterion in this case and even for frames (Ref. 52).

According to Ref. 45, "a building frame could be designed to any force level for seismic forces - as long as the building could endure the distortions involved." Although this is obviously an exaggeration, the point is made that buildings are more forgiving of stresses than distortions.

Drift limits are often used to avoid the p-delta effect in slender frames, although that effect could be evaluated rather easily. The greatest value of drift analysis is in the limitation of nonstructural (wall) damage. Furthermore, the drift limit is more of a controlling factor for stiff structures themselves with less energy absorption capacities and relatively larger forces.

Drift limits must be related to the method of analysis. Nonlinear displacements of very flexible structures can be estimated by elastic cracked section analysis, because elastic and inelastic displacements are nearly equal. The analysis of stiff structures is more difficult. If the frequency of a damaged structure is still high, the acceleration is known and the displacement can be estimated from an assumed ductility factor. Unfortunately, inelastic displacements are very sensitive to the yield strength for high-frequency structures. In the 2 to 8 Hz range the displacement increases by a factor of about $\mu \sqrt{2\mu - 1}$. The reliance on ductility factors is unfortunate but probably acceptable for low ductilities, because the inelastic displacements are small. More work needs to be done in this area.

Special characteristics of the ground motion can affect nonlinear displacements and drift. The acceleration pulse (see Chapter 2) of the Pacoima Dam input caused much larger drift (0.90%) than the El Centro motion (0.28%) in one test (Ref. 46).

It should be pointed out that in modal analysis interstory drift should be calculated for each mode separately, rather than from the combined displaced shape. Shear effects can be more pronounced in the upper stories because the dead load is smaller than in the lower stories (Ref. 36).

It has already been emphasized in Chapter 2 that one must be careful in adopting general conclusions developed mainly for flexible structures. Stiff wall-type structures can receive increasing input as the frequency reduces. Also, "an increase in initial stiffness without a reduction in tolerable story drift will lead to a considerable increase in ductility demands and therefore greater structural damage" (Ref. 59).

A recent extensive study of drift (Ref. 53) defined drift values at three levels of damage. Based on 31 sources and 215 tests (172 using concrete blocks) plus evaluation of earthquake damage, a limit of 0.5% was recommended for block walls at extensive damage levels. From a large variety of studies summarized in Ref. 53 the drift values are calculated to be: 0.15% (39 points) at "minimum tolerable level"; and 0.50% (36 points) with COV=0.65 at "maximum tolerable level". The large variation can be explained by the diversity of sources and criteria.

The eight large low-wall tests at PCA (Ref. 34) had an average drift of 0.041% (COV=0.31) at first cracking and 0.62% at failure with a low COV=0.16.

A select set of low-wall data, eight tested at PCA and 17 in Japan (Ref. 35), resulted in drifts of 0.044% (COV=0.21) at cracking and 0.55% (COV=0.31) at failure. These are good correlations with relatively small variations.

Small walls generally have more shrinkage stresses and cracks, therefore the drifts are lower at cracking. For example, based mainly on small model tests, in Japan the drift at cracking is taken at 0.022% to 0.026% (Ref. 50). The drift at failure is proposed as 0.4% based on 200 tests (Ref. 51); this value is also valid for walls with openings if $\Sigma A_o/A_{tot} < 0.25$.

The drifts at first noticeable cracking for the very small specimens tested at LANL can be estimated from the loads and reported stiffnesses (Ref. 19). For the five tests the mean is 0.057% with COV = 0.11. At failure three tests give 0.54% with COV = 0.11. As mentioned in Chapter 2, shrinkage and shear lag were significant in these tests.

Shear tests on panels, under various levels of biaxial tension, also showed a shear distortion of about 0.4% (Refs. 56, 57, and 58). The value was somewhat higher for the heavier (24-in.-thick) elements.

Damage to 59 concrete buildings in the 1971 San Fernando earthquake was studied in terms of the interstory drift r = d/h (Ref. 55). Using the approximate expression

$$r = \Gamma \frac{T}{2\pi N h} S_v.$$

For a first mode linear response and period proportional to the number of floors, $\Gamma = 1.05$ was obtained for concrete buildings. For relatively flexible structures, the drift is nearly proportional to the effective ground acceleration. The correlation between predicted and measured drifts is shown in Fig. 4-1a, whereas Fig. 4-1b depicts the percent of damage as a function of drift. A sudden increase of damage occurs for an interstory drift above about 0.6%.

To get a rough idea of the relative magnitudes of the shear stiffness and the proposed drift limits, one may assume linear behavior in pure shear up to

diagonal cracking. Then, for $\mu = 0.15$, a stress of $2\sqrt{f_c'}$, and a shear distortion of 0.1% the effective shear modulus is

$$\frac{G_{eff}}{G} = \frac{2\sqrt{f_c'}/0.001}{57{,}000\sqrt{f_c'}/2.3} = 0.080,$$

where the denominator is taken from the ACI Building Code. This ratio is rather low but not unrealistic (see Chapter 2). Note that the stress at first cracking is about twice the above value, and the distortion is probably somewhat less.

In an extensive study of various types of 3-story concrete buildings, the damage ratio in terms of total cost of repair was calculated. Inelastic dynamic analyses were conducted for a series of inputs, and the damage was calculated relative to interstory drifts and accelerations (Ref. 52). Table 4-1 shows the rapid increase of the damage ratio as the drift is increased to 1% for shear wall structures. This reference also contains information on variable damping and the coefficient of variation of ductility as a function of the period.

Nonlinear response-history analyses of a shear wall structure similar to concrete structures in nuclear facilities resulted in a maximum drift of 0.05% for a ground motion with maximum acceleration of 0.5 g (Ref. 62). At yield the drift was 0.013%. Both of these are very low values indicating that drift is probably not a problem for such box-type buildings with very heavy walls. The maximum interstory drift occurred in the top story.

Based on 179 wall tests (Ref. 49), it was found that failure forces could be prescribed with acceptable accuracy but not the deformations. An attempt was made by this author to evaluate the drifts but the variation is so large that it would be necessary to categorize the structures; this has not been done due to lack of time after the report was received. Since the amount of data is so extensive, it should be carefully analyzed.

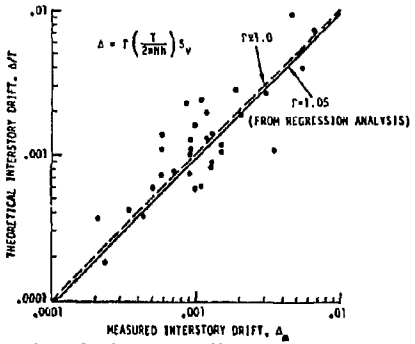

Correlation of Predicted and Measured Values of Interstory Drift for Concrete Buildings

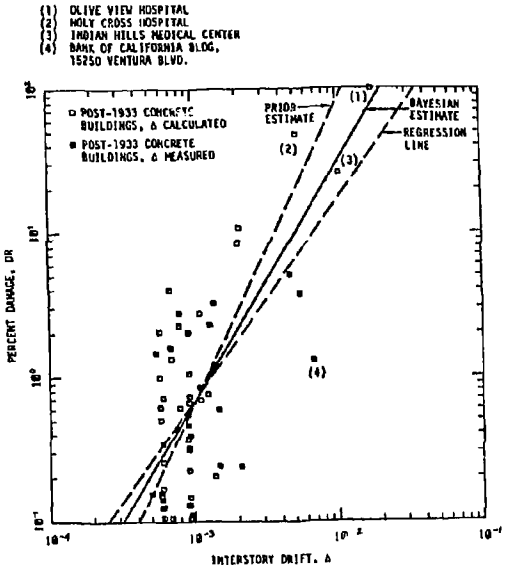

Damageability for Model for Post-1933 Reinforced Concrete Buildings, 5-20 Stories, Bayesian Estimate

Fig. 4-1 Damage vs. Drift for Concrete Building, San Fernando Earthquake

Element	Cost ($)	Repair Miltiplier	Damage Ratios for Following Interstory Drift in./in.								
			0.001	0.005	0.010	0.020	0.030	0.040	0.070	0.100	0.140
1a. Rigid Frames	117,500[a]	2.0	0	0.01	0.02	0.05	0.10	0.25	0.35	0.50	1.00
b. Braced Frames	a	2.0	0	0.03	0.14	0.22	0.40	0.85	1.0	1.0	1.0
c. Shear Walls	a	2.0	0	0.05	0.30	0.30	0.60	0.85	1.0	1.0	1.0
2a. Nonseismic Structural Frame	625,500	1.5	0	0.005	0.01	0.02	0.10	0.30	1.0	1.0	1.0
3. Masonry	417,600	2.0	0	0.10	0.20	0.50	1.0	1.0	1.0	1.0	1.0
4. Windows and Frames	120,600	1.5	0	0.30	0.80	1.0	1.0	1.0	1.0	1.0	1.0
5. Partitions, Architectural Elements	276,200	1.25	0	0.10	0.30	1.0	1.0	1.0	1.0	1.0	1.0
6. Floor	301,200	1.5	0	0.01	0.04	0.12	0.20	0.35	0.80	1.0	1.0
7. Foundation	412,100	1.5	0	0.01	0.04	0.10	0.25	0.30	0.50	1.0	1.0
8. Building Equipment and Plumbing	731,600	1.25	0	0.02	0.07	0.15	0.35	0.45	0.80	1.0	1.0
9. Contents	500,000	1.0	0	0.02	0.07	0.15	0.35	0.45	0.80	1.0	1.0

[a]varies with design

Table 4-1. Damage vs. Drift for Concrete Building, San Fernando Earthquake

The following drift limits were proposed for a variety of systems in Ref. 63.

Shear failure of short columns	0.2%
Shear failure of walls	0.4%
Flexural yielding of ductile walls	0.4%
Flexural yielding of ductile columns	0.67%

The authors recommend the origin-oriented hysteresis model for short walls.

The European concrete code for seismic loading limits the drift to 0.25% at working stress loads; otherwise nonstructural elements must be isolated from the structure (Ref. 60). The same value is given in Ref. 61 at first diagonal cracking.

In summary, measurements in the laboratory and in the field have shown that damage to stiff low walls can be related to interstory drift. At initial cracking the drift is 0.04%, at extensive diagonal cracking 0.2%, and at failure of the walls 0.4%. The coefficient of variation is about 0.30 at each of these levels. The drift at failure is almost 0.6% if high axial compression is present. Of course, drifts are much higher (at least 1%) in coupled walls and 2% if flexural yielding is present in ductile walls. Drift criteria should be used in addition to force or stress limits.

4.3 The Reserve Energy Technique

Several approaches have been developed for the estimation of inelastic behavior, or at least the dynamic capacity of structures. The key feature of most of these approximate methods is the estimation and use of a nonlinear load-deflection (lateral force-drift) relationship of the structure. As a minimum, the elastic stiffness and significant yield level are needed. Although this may seem to be and usually is a difficult task, realistic predictions of nonlinear behavior are impossible without this information.

The reserve energy technique (RET) has been developed by J. A. Blume and described in several publications (for example Ref. 62). An energy balance is set up

$$E_I = E_D + E_R$$

where E_I = energy input, E_D = energy dissipated, E_R = energy radiated away.

The demand $E_D = E_I - E_R$ is estimated by linear analysis. The capacity is equal to the area of the force-deflection diagram. This iterative method results in the maximum inelastic story distortions (Ref. 62) and local ductilities.

The RET has been found to be an attractive tool for the estimation of nonlinear response. For complex structures with extensive force redistribution, an iterative analysis is required but the method is still much simpler than direct nonlinear analysis and, at the same time, keeps the actual behavior and any peculiarities in good focus. It can predict local nonlinearities as opposed to the ductility-based spectrum method (Chapter 2).

4.4 The Capacity Spectrum Method

In this approach the demand and capacity spectra are superposed and the solution is obtained at their intersection (Ref. 64). The capacity curve is determined from a linear analysis up to appreciable yield and by an inelastic or piece-wise linear analysis beyond significant yielding. The stiffness is reduced every time a group of plastic hinges form. For each stage of response the period, mode shape, participation factor, spectral acceleration and spectral displacement are calculated.

For each stage of the piecewise linear base shear(V)-roof displacement (d_R) relationship the first-mode period, mode shape (ϕ), and participation

factors (Γ) are calculated. The spectral displacements S_d are evaluated from the relationship,

$$d_r = \Gamma \phi_r S_d.$$

The corresponding spectral accelerations are obtained from

$$C_b = \frac{V}{W} = \frac{\sum m\phi}{M} a\Gamma,$$

where W and M are the total weight and mass, C_b is the base shear coefficient, and $a = S_a/g$ is the spectral acceleration coefficient. The capacity curve, S_a versus S_d, can be plotted, as illustrated in Fig. 4-2a.

The periods are

$$T = 2\pi \sqrt{\frac{S_d}{S_a}},$$

and the capacity spectrum curve may be superposed on the earthquake spectrum curve (Fig. 4-2c). Finally, an interpolation of the input curves for two values of damping, one for elastic and the other at high-level response, defines a straight line, and its intersection with the capacity spectrum is the solution. The damage level and distortions are readily available.

4.5 The Substitute Structure Methods

Equivalent single-degree systems to predict the nonlinear response of certain types of structures have been proposed by several researchers. In the "substitute structure method" (Ref. 66) the nonlinear properties are reflected by reduced stiffnesses and hysteretic energy absorption by an equivalent damping. This method has been used successfully either to calculate the required yield resistance for given damage (ductility) ratios and initial stiffnesses or to estimate the damage (drift) for given yield capacities and stiffnesses (Ref. 67).

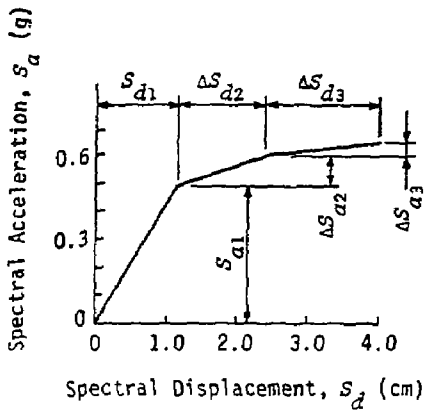

(a) CAPACITY: SPECTRAL ACCELERATION VERSUS SPECTRAL DISPLACEMENT

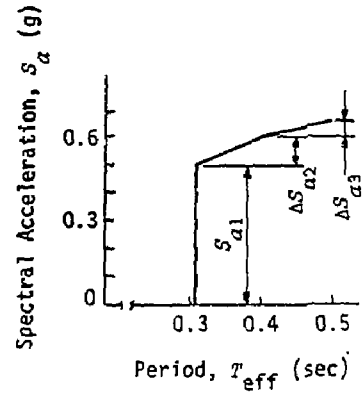

(b) CAPACITY: SPECTRAL ACCELERATION VERSUS EFFECTIVE PERIOD

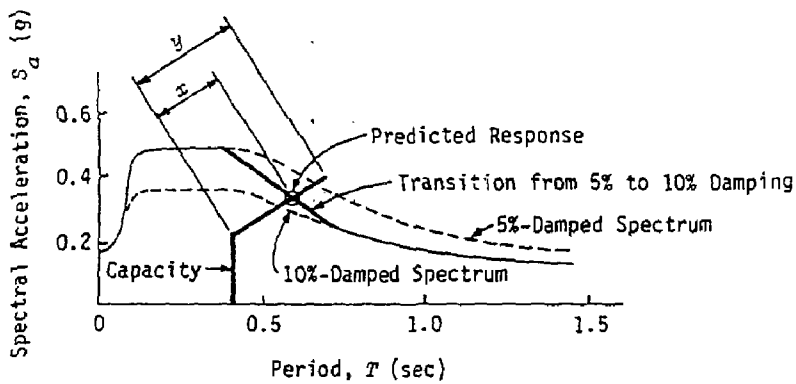

(c) CAPACITY AND DEMAND, SPECTRAL ACCELERATION VERSUS PERIOD

Fig. 4-2 The Capacity Spectrum Method

In the Q-model the equivalent single-degree system has hysteretic properties and a nonlinear time-response analysis is required (Ref. 68). In a recent version a static limit analysis of the structure is used to establish the nonlinear response of the model (Ref. 69).

The common assumptions and characteristics of these approaches are that the response can be adequately described by the first mode shape and planar behavior, the structure is flexible (acceleration decreases with increase in period), and the input is of the El Centro or Taft type. It is not known how these methods can be extended to stiff, walled structures. Some information on the application of all methods, except the Q-model, to the structure types of interest is contained in Ref. 62. It appears that the substitute structure method and the capacity spectrum method overestimate the ductility demand for stiff structures.

It is not clear how much can be expected from simplified methods for stiff (high-frequency) structures whose response (inelastic displacement) is very sensitive to the yield capacity and the details of the ground motion. More work needs to be done in this area because the alternative, that is, nonlinear response-history analysis, is not much more reliable.

4.6 Inelastic Response Spectrum Approach

All the previous methods discussed in this chapter use the elastic response spectrum (or a response-history analysis for the Q-model). The use and the limitations of the ductility-based reduced spectrum have been discussed in Chapter 2.

4.7 Nonlinear Response-History Analysis

The approximate methods outlined in previous sections were developed to avoid using direct nonlinear analysis. It is well known that nonlinear analyses of large systems require extensive computer costs and are not practical except in unusual cases.

However, several factors would make nonlinear response-history analyses of doubtful value even if the cost of analysis were not a problem; this is especially true for high-frequency structures. Among the most significant uncertianties in nonlinear response-history analyses are: definition of hysteresis curves for all types of deterioration and as functions of axial load; change of damping during response; soil-structure interaction; effect of input characteristics; role of nonstructural elements; and floor deformations.

Most of these factors are especially important for stiff structures where the ductility demand is highly variable. It is generally agreed that the details of the ground motion greatly influence nonlinear response and that artificial inputs should not be used. A variety of recorded motions must be applied to evaluate this factor. Multi-directional inputs also affect nonlinear response much more than linear response (Ref. 70).

Although nonlinear dynamic analyses are valuable tools for research, especially in substantiating simplified methods, and in studying specific factors, they are not yet suitable for the design or analysis of complex structures or in probabilistic risk assessment.

4.8 Summary

Several approximate methods of nonlinear analysis were outlined in this chapter. A common feature of most of these approaches is the need to construct a static nonlinear force-displacement curve. They have been developed mainly for low-frequency structures and more work is necessary before these powerful tools can be used for the analysis of high-frequency structures.

Drift limits were recommended at various damage states of wall structures as analysis criteria to be used in addition to stress limits.

5 RECOMMENDATIONS

Although the SSMRP has produced a useful analysis procedure that is able to identify uncertainties and evaluate the effects of parameters, several constituents require improvements and additional studies. This is not surprising because of the sophistication and precision required in probabilistic risk assessment relying on the state of the art in modeling, input definition, and analysis.

The following items require additional work to make fragility analysis a more reliable tool. These recommendations are listed in approximate order of importance.

1. Realistic predictions of nonlinear response require the knowledge of the progress of inelasticity throughout the structure; this cannot be bypassed or avoided. It is necessary to construct static nonlinear load-displacement relationships for the structure but, as a minimum, for each story. These curves will shed light on the failure sequence and load redistribution. In addition, they will greatly help in calculating system ductilities from member ductilities and reveal the effects of inelasticity on torsion. Static load-displacement curves form the bases of most approximate nonlinear analysis models (Chapter 4).

2. Most simplified analytical methods and test programs have concentrated on low-frequency structures. Many observations and established procedures are not expected to apply to high-frequency wall structures. The response may increase as the frequency reduces during motion. The inelastic displacements are very sensitive to the yield level as opposed to being nearly equal to the elastic displacements for flexible structures. Furthermore, the effects of the peculiarities of near-field ground motions are more severe for stiff structures and the number of cycles is greater. These differences must be investigated because they apply to concrete structures in nuclear facilities; the results should be useful not only to probabilistic risk assessment (PRA) but also to seismic analysis in

general. Not enough is known about the response of structures on the high-frequency side of the peak of the spectrum curve, especially for nonlinear behavior.

3. Nonlinear structural actions influence in-structure response spectra and may lead to higher spectral values in certain frequency ranges. Although several investigations have already addressed this question, satisfactory solutions appropriate for PRA are not available, especially for high-frequency systems. A three-pronged study is recommended involving direct nonlinear analysis, evaluation and analysis of experimental floor responses, and analysis by approximate nonlinear models.

4. Diaphragms in nuclear facilities normally have many randomly-placed holes. Little is known about the nonlinear behavior (stiffness and failure) of such floor diaphragms due to in-plane shear, bending, and tension. A combined analytical (finite element) and experimental study is needed to generate analytical tools for safety assessment. A secondary problem is the strength of the connections of diaphragms to supporting elements.

5. More experimental information is needed on the stiffness and strength of low shear walls not affected much by flexure. Some of the tests should have embedded steel frames with or without studs. Tests are also required on multistory, multi-bay walls to calibrate analytical procedures and to study frame-wall interaction and the role of embedded columns. As a minimum, all available tests, especially from Japan, should be reanalyzed with special attention to failure modes of low walls.

6. The fragility curves were calculated for constant system ductilities and high levels of damping. As discussed in Chapter 2, a rational improvement would be to vary the ductility and damping as a function of the input level and the target damage level. This reanalysis could be done without extensive effort and, at the same time, more realistic lower damping values could be selected.

7. The out-of-plane bending and failure of walls (and floors) have been common in earthquakes, yet little information is available. A thorough experimental investigation is urgently needed that should include reinforced concrete and masonry walls subjected to inertia loading.

8. Ductility-based reduced spectra were not found to depend a lot on the shape of the hysteresis curve. However, shear deformations of walls cause severe pinching of the hysteresis curves which was not included in the original Newmark study. It is necessary to extend the Newmark-Riddell work to such systems and, at the same time, to high-frequency structures and near-field inputs with large acceleration pulses. It is expected that the deamplification will be different and more variable.

9. Several simple models have been developed for the analysis of structures (see Chapter 4). However, these are probably not applicable to high-frequency structures. It seems desirable to develop such substitute models because they permit parametric studies of variables; one of them is the topical question of the effects of acceleration pulses in ground motions on nonlinear response. Another important problem is nonlinear response as a result of multi-directional inputs, which can be more severe than elastic response. A limited amount of nonlinear dynamic analysis would also be worthwhile.

10. Critical items may be attached to walls. An evaluation of available information, supplemented by testing, is needed to establish the pullout safety of anchors in diagonally cracked walls at various stages of damage.

11. The fragility curves in the SSMRP were established for in-structure response parameters. This has computational advantages and is reasonably consistent for linear behavior. The transmission of energy from the ground to the selected point in the structure and to various elements would depend on the nature of nonlinearity, ground motion characteristics, and other factors if inelasticity were directly considered.

12. The roof of the turbine building is made of precast concrete slab elements with little or no interconnections. They may buckle due to in-plane inertia forces causing compression and bending; the pieces would then fall to the floor below. Analytical models of such systems should be established and validated experimentally.

13. The probability of yielding or fracture of reinforcing bars embedded in concrete is smaller than that without concrete (Section 2.5). A recent study by the author has shown that little is known about this effect. An experimental program is needed to supply data for some improvement in the fragility numbers, though this factor is less important than those mentioned previously.

6 SUMMARY AND CONCLUSIONS

Fragility analysis, that is the construction of cumulative distribution functions of the probability of failure of critical elements, is evaluated in this report. The development of fragility analysis is part of the Seismic Safety Margins Research Program (SSMRP). The principal attribute of the SSMRP is the calculation of uncertainties in dynamic response, ranging from the input to material behavior and failure levels.

The main emphasis in this report is on the validation of the idealization and analytical description of the behavior of reinforced concrete elements, but associated analytical steps are also discussed. Low shear walls receive particular attention because they are critical and prevalent in nuclear facilities.

Probabilistic risk assessment is evaluated in general and also as applied to the analysis of the Zion plant. Specific questions examined in detail include: the use of ductility-based reduced spectra and the associated damping values, uncertainties in material modeling, initial stiffness and strength of shear walls, certain specific failure modes, and alternative nonlinear analysis techniques.

The following are the main conclusions of this report:

1. Fragility analysis can serve an important role in risk assessment, because it purports to quantify the effects of uncertainties and risk levels.

2. Probabilistic risk assessment and fragility analysis require best estimates and the calculation of variations of input values which are much more difficult tasks than the usual goal of just a safe design. Information necessary to make best estimates is often rather limited, and the data can easily be misinterpreted.

3. Static nonlinear (piecewise linear) analysis would generate essential information and is strongly recommended as part of seismic risk or other extreme load risk analysis. Such an analysis would greatly aid in the calculation of system ductilities, load redistribution after nonlinearities develop, and in the identification of the second line of defense. Most approximate nonlinear analysis methods utilize static force-deflection curves.

4. Approximate inelastic analysis methods are preferable to direct response-history analyses for routine applications because the latter involve too many uncertainties. The ductility-based reduced spectrum method, which was used in the SSMRP, is one such method but other approaches also show potential; some are reviewed in Chapter 4. These include the substitute structure method, the capacity spectrum method, and the reserve energy technique. The main feature of most approximate methods is the use of the static nonlinear force-curve and the elastic spectrum with a shift in the natural frequencies.

5. The basic problem with the ductility-based spectral analysis is the calculation of system ductility from local ductilities and vice versa. The critical wall stresses were reduced using a system ductility, which was related to individual wall ductilities, but the former depends on the aggregate effects of local ductilities.

6. The ductility and damping factors were assumed to be constant. An improved risk assessment would result from the use of ductilities and damping that would depend on the response level; the changes could be made without extensive effort.

7. An extensive review and analysis of wall test results has revealed that most available information on walls relates to tall walls in which bending is significant. The walls in nuclear plants are normally very low, and flexural equations do not apply. A set of two equations is proposed to predict the strength of low walls that were

found to be critical elements in most nuclear facilities. One was derived from the compression field theory, and the other is based on the equation developed in the SSMRP and includes the contributions of horizontal and vertical reinforcement. The predicted/measured ratio is 0.99 with a coefficient of variation of 0.26 (Section 2.6). In addition, drift limits are recommended for the prediction of three damage limit states of low walls (Section 4.2).

8. A ductility of four was used for local respose of walls and a value of two for system ductility. The former number is more representative of flexural walls and is too high for low walls. The derivation of system ductility and its use in the prediction of local stresses in critical elements needs improvements (see Item 5). Also, shear-dominated walls have highly pinched hysteresis loops which are not reflected in Newmark's ductility-based spectra, especially in the high-frequency region. This key step in the SSMRP needs further study.

9. The use of high damping ratios (about 10%) in conjunction with ductility-based spectral reduction represents a duplication of hysteretic energy absorption. A lower level of viscous damping (about 2% to 6%) is recommended if hysteresis is accounted for by the use of ductility factors. Fortunately, the results are not affected much by damping for high-frequency structures.

10. The initial stiffness directly affects frequencies and modal analysis. An extensive study of measured wall stiffnesses revealed great variations, from about 0.20 to 0.80 times the uncracked stiffness. These differences are explained, and recommended stiffnesses with coefficients of variation are presented in Section 2.5. It is claimed that it is difficult and probably impossible to use small models to simulate the initial behavior of large walls because of shrinkage, vertical load, and bond effects. In box-type wall systems the shear lag effects may also be appreciable.

11. Nonlinear response depends, more than linear response, on the characteristics of the gound motion. This is especially true for high-frequency (wall) structures near the seismic source. Therefore, it is insufficient to use only artifical ground motions that do not have these special properties.

12. Mode combination rules are suggested that include the effects of damping on modal correlation.

13. Several additional material uncertainties were analyzed, and coefficients of variations are reported.

14. The failure of the main wall between the auxiliary and turbine buildings of the Zion plant contains an embedded steel frame. The failure of the studs on the frame was assumed to be sudden, resulting in a transfer from shear behavior to flexural action of separated slender walls which would fail at a low load. However, review of the force transfer mechanism and stud behavior has led to a different stress distribution and a model with gradual stiffness loss.

15. The role of nonstructural walls, which were ignored in the fragility analysis because additional stiffness would result in reduced response, needs further study. Their effect on the response, especially on torsional response, initially and after deterioration, may be significant. Walls also affect damping, especially after cracking.

It is difficult to see what the final implications of fragility curves are. Eventually one needs to relate them back to the ground motion to assess the probability, feasibility, and consequences of each level of ground motion. This step would also aid in the curtailment of the tails of the fragility curves.

Nuclear power plants are so complex and varied that fragility analysis (and PRA) cannot become a routine, general, and foolproof tool. It will be necessary to rely on expert advice and insight in the evaluation of nonlinear behavior and failure modes of critical structural components to avoid erroneous idealizations, assumptions, and misuse.

Although the SSMRP has represented a significant step in the state of the art of seismic risk assessment of structures, especially in the area of soil-structure interaction, additional analytical and experimental work is recommended. Chapter 5 contains the recommendations.

7 REFERENCES

1. P. D. Smith, et. al., Seismic Safety Margins Research Program Phase I Final Report, Vol. 1-10, NUREG/CR-2015, (1981, 1982).

2. D. A. Wesley and P. S. Hashimoto, Seismic Structural Fragility Investigation for the Zion Nuclear Power Plant, SSMRP Phase I, NUREG/CR-2320,(1981).

3. P. Gergely, Structural Dynamics and Introductior to Earthquake Engineering, manuscript to be published in 1984.

4. M. P. Bohn, et. al., Application of the SSMRP Methodology to the Seismic Probabilistic Risk Analysis at the Zion Nuclear Power Plant, SMIRT, Chicago, Illinois, (August 1983.)

5. V. V. Bertero, et. al., Establishment of Design Earthquakes-Evaluation of Present Methods, Int. Symposium on Earthquake Structural Engineering, St. Louis, Missouri, (1976.)

6. P. Muellier, Private communication, 1983.

7. T. F. Zahran and W. J. Hall, Seismic Energy Absorption in Simple Structures, SRS 501, University of Illinois, (1982.)

8. S. A. Mahin and V. V. Bertero, An Evaluation of Inelastic Seismic Design Spectra, ST9, ASCE, (Sept. 1981.)

9. R. Riddell and N. M. Newmark, Statistical Analysis of the Response of Nonlinear Systems Subjected to Earthquakes, SRS 468, University of Illinois, (1979).

10. R. P. Kennedy, Peak Acceleration as a Measure of Damage, 4th International Seminar on Extreme-Load Design of Nuclear Power Facilities, Paris, France (August 1981.)

11. W. D. Iwan and N. C. Gates, "The Effective Period and Damping of a Class of Hysteretic Structures", Earthquake Engineering and Structural Dynamics, Vol. 7, 199-211, (1979).

12. M. Celebi, On the Shear Pinched Hysteresis Loops, International Symposium on Earthquake Structure Engineering, St. Louis, Missouri, (1976).

13. T. Shiga, et. al., Experimental Study on Dynamic Properties of Reinforced Concrete Shear Walls, 5th World Conference on Earthquake Engineering, Rome, Italy, (1973).

14. R. G. Oesterle, et. al., Free Vibration Tests of Structural Walls, 7th World Conference of Earthquake Engineering, New Delhi, India, (1980).

15. T. M. Ferritto, An Evaluation of Inelastic Response in Predicting Ductility Demands, TM 51-80-21, CEL, Naval Construction Battalion Center, Port Hueneme, (1980).

16. S. A. Mirza, et. al., Statistical Descriptions of Strength of Concrete, ASCE, ST6, (June 1979).

17. International Workshops on Shear and Torsion in Concrete, P. Gergely organizer, Zurich 1981, Quebec 1982, Munich, West Germany, (1982).

18. S. A. Mirza, et. al., Variability of Mechanical Properties of Reinforcing Bars, ST5, ASCE, (1979).

19. E. G. Endebrock, Preliminary Report, Category I Program, FY 83, Los Alamos National Laboratory, Los Alamos, New Mexico, (1983).

20. P. Ferguson, Fundamentals of Reinforced Concrete, Prentice-Hall, (1973).

21. J. D. Aristizabal-Ochoa, Behavior of Ten-Story Reinforced Concrete Walls Subjected to Earthquake Motion, Vol. 1, SRS 431, (1976).

22. Personal Communications from A. Aktan, K. Sakino, and V. Bertero, University of California, Berkeley, 1983.

23. R. N. White and P. Gergely, Shear Transfer in Thick-Walled Reinforced Concrete Structures under Seismic Loading, Cornell University, Dept. of Structural Engineering, No. 78-2, (1978).

24. H. Umemura, et. al., Aseismic Characteristics of RC Box and Cylinder Walls, 6th World Conf. Earthquake Energy, New Delhi, India (1977).

25. J. D. Aristizabal-Ochoa, Cracking and Shear Effects in Structural Walls, ST5, ASCE, (May 1983).

26. Paper manuscript from A. E. Aktan and V. V. Bertero, University of California, Berkeley, 1983.

27. S. A. Freeman, et. al., Dynamic Response Investigations of Real Buildings, Earthquake-Resistant Reinforced Concrete Building Construction, UC Berkeley, Vol. III, (1977).

28. R. L. Mayes and T. V. Galambos, Large-Scale Dynamic Shaking of 11-Story Reinforced Concrete Building, UC Berkeley, Vol. III, (1977).

29. G. C. Hart and R. Vasudevan, Earthquake Design of Buildings: Damping, ST1, ASCE, (Jan. 1975).

30. Seismic Resistence of RC Shear Walls and Frame Joints, Preliminary draft, ATC-11, Applied Technology Council, Palo Alto, (1983).

31. P. Gergely, Experimental and Analytical Investigations of RC Frames Subjected to Earthquake Loading, ERRCBC (see Ref. 27), Vol. III, (1977).

32. M. P. Collins, A Note on the Failure Criterion for Diagonally Cracked Concrete, ERRCBC (see Ref. 27), Vol. III, (1977).

33. R. G. Oesterle, et. al., Web Crushing of Reinforced Concrete Structural Walls, unpublished manuscript, PCA, (1983).

34. F. J. Barda, et. al., Shear Strength of Lowrise Walls with Boundary Elements, Reinforced Concrete Structures in Seismic Zones, ACI, SP53, Detroit, Michigan, (1976).

35. T. Shiga, "Hysteretic Behavior of Reinforced Concrete Shear Walls", Proc. US-Japan Cooperative Research, The Safety of School Buildings, Hawaii, (1975).

36. R. Iliya and V. V. Bertero, Effects of Amount and Arrangement of Wall-Panel Reinforcement on Hysteretic Behavior of Reinforced Concrete Walls, University of California, Berkeley, UCB/EERC-80/04, (1980).

37. T. Paulay, et. al., "Ductility in Earthquake Resisting Squat Shearwalls," ACI Journal, Vol. 79, (July-August 1982.)

38. R. D. Campbell and D. A. Wesley, Potential Seismic Structural Failure Modes Associated with the Zion Nuclear Plant, SSMRP, NUREG/CR-1704, (1981).

39. D. S. Neille, "Behavior of Headed Stud Connections for Precast Concrete Panels and Monotonic and Cycled Shear Loading", Structural Research Series No. 20, The University of British Columbia, Canada, (1977).

40. Structural Design of Tall Steel Buildings, Planning and Design of Tall Buildings, Vol. SB, Chapter 9, ASCE, (1979).

41. R. A. Spencer and D. S. Neille, "Cyclic Tests of Welded Headed Stud Connections", Journal of PCI, Vol. 21, No. 3, (May 1976).

42. R. N. White and P. Gergely, Shear Transfer in Thick-Walled Reinforced Concrete Structures under Seismic Loading, No. 75-10, Dept. of Structural Engineering, Cornell University, (1975).

43. P. Gergely and J. K. Smith, "Seismic Response of Cracked Cylindrical Concrete Structures," Proc. U.S. National Conference on Earthquake Engineering, Stanford University, (August 1979).

44. C. H. Conley, et. al., Analysis of R/C Containment Vessels with Nonlinear Shearing Stiffness, Dept. of Structural Engineering, Cornell University, NUREG/CR-3255, (1983).

45. R. N. White and P. Gergely, "Peripheral (Punching) Shear Strength of Biaxially Tensioned R/C Wall Elements", 6th SMiRT, Paris, 1981, or Nuclear Engineering and Design, Vol. 69, (1982).

46. E. J. Teal, "Seismic Drift Control and Building Periods", Engineering Journal, AISC, (February, 1978).

47. A. E. Aktan, et. al., Prediction of the Seismic Responses of R/C Frame - Coupled Wall Structures, UCR/EERC 82/12, Berkeley, (August 1982).

48. V. V. Bestero and B. Bresler, Panel on Design and Engineering Decisions: Failure Criteria (Limit States), Panel discussion, 6th World Conference on Earthquake Engineering, New Delhi, India, (1977).

49. M. Hirosawa, Past Experimental Results on Reinforced Concrete Shear Walls and Analysis on Them, Building Research Institute, No. 6, pp. 277, (March 1975).

50. K. Yoshimura, Research on R/C Shear Walls in Japan, personal communication to V. V. Bertero and A. E. Aktan, 1982.

51. M. Tomii and M. Takeuchi, "The Relations Between the Deformation Angle and the Shearing Force Ratio, with Regard to 200 Shear Walls", Trans. Arch. Inst. Japan, No. 153, (1968).

52. J. M. Ferritto, An Economic Analysis of Earthquake Design Levels, Naval Civil Engineering Laboratory, TN-1640, July 1982 and TN-1671, (July 1983).

53. B. B. Algan, Drift and Damage Considerations in Earthquake - Resistant Design of R/C Buildings, Ph.D. thesis, University of Illinois at Urbana-Champaign, (1982).

54. H. Banon, et. al., Seismic Damage in Reinforced Concrete Frames, ST9, ASCE, (1981).

55. T. K. Hasselman and J. K. Wiggins, "Earthquake Damage to Highrise Buildings as a Function of Interstory Drift", 3rd International Earthquake Microzonation Conf., Seattle, Vol. II, (1983).

56. P. C. Perdikaris, et. al., Strength and Stiffness of Tensioned R/C Panels Subjected to Membrane Shear; Two-Way Reinforcing, Dept. of Structural Eng., Cornell University, NUREG/CR-1602, (1980).

57. R. G. Oesterle and H. G. Russell, Shear Transfer in Large Scale R/C Containment Elements, NUREG/CR-1374, (1980).

58. F. Vecchio and M. P. Collins, The Response of Reinforced Concrete to In-Plane Shear and Normal Stresses, Dept. of Civil Engineering, University of Toronto, No. 82-03, (1982).

59. V. V. Bertero and B. Bresler, "Serviceability Drift Limits for Essential Facilities", 6th World Conf. Earthquake Engineering, New Delhi, India, (1977).

60. Seismic Design of Concrete Structures, Comite Euro-Internatinal du Beton, CEB, No. 149, (1982).

61. Structural Design of Tall Concrete Buildings, Planning and Design of Tall Buildings, Vol. CB, ASCE, (1979).

62. Nonlinear Structural Dynamic Analysis Procedures for Category I Structures, URS/John A. Blume Associates, NUREG/CR-0948, (1979).

63. H. Aoyama and S. Otani, Recent Japanese Developments in Earthquake Resistant Design of R/C Buildings, C. P. Siess Symposium, ACI, (1979).

64. S. A. Freman; "Prediction of Response of Concrete Buildings to Severe Earthquake Motion," Proc., McHenry Symposium, ACI, (1977).

65. S. A. Freeman, et. al., Seismic Design Guidelines for Essential Buildings, paper manuscript, (1983).

66. A. Shibata and M. A. Sozen, Substitute Structure Method for Seismic Design in R/C, ASCE, ST1, (1976).

67. A. W. F. Metten, et. al., "Pseudo-Nonlinear Modal Analysis of Coupled Shear Walls", 4th Canadian Earthquake Engineering, Proc., Vancouver, British Columbia, Canada,(June 1983).

68. M. Saiidi and M. A. Sozen, Simple Nonlinear Seismic Analysis of R/C Structures, ASCE, ST12, (1981).

69. M. Saiidi and K. E. Hodson, "Earthquake Response of Irregular R/C Structures in the Nonlinear Range", Computers and Structures, Vol. 16, No. 1-4, (1983).

70. D. A. Pecknold, Inelastic Structural Response to 2D Ground Motion, ASCE, EM5, (1974).

71. B. Ellingwood, Probabilistic Descriptions of Resistance of Safety-Related Nuclear Structures, NUREG/CR-3341, (1983).

72. D. A. Wesley and P. S. Hashimoto, Preliminary Evaluation of Nonlinear Seismic Response Effects for Nuclear Power Plant Shear Wall Structures, Draft, SMA 12205.02, for Lawrence Livermore Laboratory, (1980).

73. V. Tansirikongkol and D. A. Pecknold, Approximate Modal Analysis of Bilinear MDF Systems, ASCE, EM2, (1980).